



1    Comparative geochemical study on Furongian (Toledanian) and Ordovician  
2    (Sardic) felsic magmatic events in south-western Europe

3

4    J. Javier Álvaro<sup>a\*</sup>, Teresa Sánchez-García<sup>b</sup>, Claudia Puddu<sup>c</sup>, Josep Maria Casas<sup>d</sup>,  
5    Alejandro Díez-Montes<sup>e</sup>, Montserrat Liesa<sup>f</sup> & Giacomo Oggiano<sup>g</sup>

6

7    <sup>a</sup> *Instituto de Geociencias (CSIC-UCM), Dr. Severo Ochoa 7, 28040 Madrid, Spain,*

8    *jj.alvaro@csic.es*

9    <sup>b</sup> *Instituto Geológico y Minero de España, Ríos Rosas 23, 28003 Madrid, Spain,*

10    *t.sanchez@igme.es*

11    <sup>c</sup> *Dpto. Ciencias de la Tierra, Universidad de Zaragoza, 50009 Zaragoza, Spain,*

12    *claudiapuddugeo@gmail.com*

13    <sup>d</sup> *Dpt. de Dinàmica de la Terra i de l'Oceà, Universitat de Barcelona, Martí Franquès*

14    *s/n, 08028 Barcelona, Spain, casas@ub.edu*

15    <sup>e</sup> *Instituto Geológico y Minero de España, Plaza de la Constitución 1, 37001*

16    *Salamanca, Spain, al.diez@igme.es*

17    <sup>f</sup> *Dept. de Mineralogia, Petrologia i Geologia aplicada, Universitat de Barcelona, Martí*

18    *Franquès s/n, 08028 Barcelona, Spain, mliesa@ub.edu*

19    <sup>g</sup> *Dipartimento di Scienze della Natura e del Territorio, 07100 Sassari, Italy,*

20    *giacoggi@uniss.it*

21

22    \* Corresponding author

23



24     **ABSTRACT**

25

26     A geochemical comparison of Early Palaeozoic felsic magmatic episodes throughout  
27     the south-western European margin of Gondwana is analysed. The comparison is  
28     made between (i) Furongian–Early Ordovician (Toledanian) activities recorded in the  
29     Central Iberian and Galicia-Trás-os-Montes Zones of the Iberian Massif, and (ii) Early–  
30     Late Ordovician (Sardic) activities in the eastern Pyrenees, Occitan Domain (Albigeois,  
31     Montagne Noire and Mouthoumet massifs) and Sardinia. Both phases are related to  
32     uplift and denudation of an inherited palaeorelief, and stratigraphically preserved as  
33     distinct angular discordances and paraconformities involving gaps of up to 30 m.y. The  
34     geochemical features of the Toledanian and Sardic, felsic-dominant activities point to a  
35     predominance of byproducts derived from the melting of metasedimentary rocks, rich in  
36     SiO<sub>2</sub> and K<sub>2</sub>O and with peraluminous character. Zr/TiO<sub>2</sub>, Zr/Nb, Nb/Y and Zr vs. Ga/Al  
37     ratios, and REE and  $\epsilon$ Nd values suggest the contemporaneity, for both phases, of two  
38     geochemical scenarios characterized by arc and extensional features evolving to  
39     distinct extensional and rifting conditions associated with the final outpouring of mafic  
40     tholeiitic-dominant lava flows. The Toledanian and Sardic phases are linked to neither  
41     metamorphism nor penetrative deformation; on the contrary, their unconformities are  
42     associated with foliation-free open folds subsequently affected by the Variscan  
43     deformation. The geochemical and structural framework precludes a subduction  
44     scenario reaching the crust in a magmatic arc to back-arc setting, but favours partial  
45     melting of sediments and/or granitoids in a continental lower crust triggered by the  
46     underplating of hot mafic magmas during extensional events related to the opening of  
47     the Rheic Ocean.

48     **Keywords:** granite, orthogneiss, geochemistry, Cambrian, Ordovician, Gondwana.

49

50



51    **1. Introduction**

52

53    A succession of stepwise Early–Palaeozoic magmatic episodes, ranging in age from  
54    Furongian to Late Ordovician, is widespread along the south-western European margin  
55    of Gondwana. Magmatic pulses are characterized by their preferential development in  
56    different palaeogeographic areas and linked to the development of stratigraphic  
57    unconformities, but they are related to neither metamorphism nor penetrative  
58    deformation. In the Central Iberian Zone of the Iberian Massif (representing the western  
59    branch of the Ibero-Armorican Arc), this magmatism is mainly represented by the Ollo  
60    de Sapo Formation, which has long been recognized as a Furongian–Early Ordovician  
61    (495–470 Ma) assemblage of felsic-dominant volcanic, subvolcanic and plutonic  
62    igneous rocks. This magmatic activity is contemporaneous with the development of the  
63    Toledanian Phase, which places Lower Ordovician (upper Tremadocian–Floian) rocks  
64    onlapping an inherited palaeorelief formed by Ediacaran–Cambrian rocks and involving  
65    a sedimentary gap of ca. 22 m.y. This unconformity can be correlated with the  
66    “Furongian gap” identified in the Ossa-Morena Zone of the Iberian Massif and in the  
67    Anti-Atlas Ranges of Morocco (Álvaro et al., 2007, 2018; Álvaro and Vizcaíno, 2018;  
68    Sánchez-García et al., 2019) and with the “lacaune normande” in the central and  
69    North-Armorican Domains (Le Corre et al., 1991).

70       Another felsic-dominant magmatic event, although younger (Early–Late Ordovician)  
71    in age, has been recognized in some massifs situated along the eastern branch of the  
72    Variscan Ibero-Armorican Arc, such as the eastern Pyrenees, the Occitan Domain and  
73    Sardinia. This magmatism is related to the Sardic unconformity, where Furongian–  
74    Lower Ordovician rocks are unconformably overlain by those attributed to the  
75    Sandbian–lower Katian (former Caradoc). The Sardic Phase is related to a  
76    sedimentary gap of ca. 16–20 m.y. and geometrically ranges from 90° (angular  
77    discordance) to 0° (paraconformity) (Barca and Cherchi, 2004; Funneda and Oggiano,  
78    2009; Álvaro et al., 2016, 2018; Casas et al., 2019).



Although a general consensus exists to associate this Furongian–Ordovician magmatism with the opening of the Rheic Ocean and the drift of Avalonia from northwestern Gondwana (Díez Montes et al., 2010; Nance et al., 2010; Thomson et al., 2010; Álvaro et al., 2014a), the origin of this magmatism has received different interpretations. In the Central Iberian Zone, for instance, proposals point to: (i) magmas formed in a subduction scenario reaching the crust in a magmatic arc to back-arc setting (Valverde-Vaquero and Dunning, 2000; Castro et al., 2009); (ii) magmas resulting from partial melting of sediments or granitoids in a continental lower crust affected by the underplating of hot mafic magmas during an extensional regime (Bea et al., 2007; Montero et al., 2009; Díez Montes et al., 2010); and (iii) magmas formed by post-collisional decompression melting of an earlier thickened continental crust, and without significant mantellic involvement (Villaseca et al., 2016). In the Occitan Domain (southern French Massif Central and Mouthoumet massifs) and the eastern Pyrenees, Marini (1988), Pouclet et al. (2017) and Puddu et al. (2019) have suggested a link to mantle thermal anomalies. Navidad et al. (2018) proposed that the Pyrenean magmatism was induced by progressive crustal thinning and uplift of lithospheric mantle isoterms. In Sardinia, Oggiano et al. (2010), Carmignani et al. (2001), Gaggero et al. (2012) and Cruciani et al. (2018) have suggested that a subduction scenario, mirroring an Andean-type active margin, originated the main Mid–Ordovician magmatic activity. In the Alps, the Sardic counterpart is also interpreted as a result of the collision of the so-called Qaidam Arc with this Gondwanan margin, subsequently followed by the accretion of the Qilian Block (Von Raumer and Stampfli, 2008; Von Raumer et al., 2013, 2015). This geodynamic interpretation is mainly suggested for the Alpine Briançonnais-Austroalpine basement, where the volcanosedimentary complexes postdating the Sardic tectonic inversion and folding stage portray a younger arc-arc oblique collision (450 Ma) of the eastern tail of the internal Alpine margin with the Hun terrane, succeeded by conspicuous exhumation in a transform margin setting (430 Ma)



106 (Zurbiggen et al., 1997; Schaltegger et al., 2003; Franz and Romer, 2007; Von  
107 Raumer and Stampfli, 2008; Von Raumer et al., 2013; Zurbiggen, 2015, 2017).

108 Till now the Toledanian and Sardic magmatism had been studied and interpreted  
109 separately on different areas without taking into account their similarities and  
110 differences. In this work, the geochemical affinities of the Furongian–Early Ordovician  
111 (Toledanian) and Early–Late Ordovician (Sardic) felsic magmatic activities recorded in  
112 the Central Iberian and Galicia-Trás-os-Montes Zones, Pyrenees, Occitan Domain and  
113 Sardinia are compared. This re-appraisal may contribute to a better understanding of  
114 the meaning and origin of this stepwise magmatism, and thus, to discuss the  
115 geodynamic scenario of this Gondwana margin (Fig. 1A) during Cambrian–Ordovician  
116 times, bracketed between the Cadomian and Variscan orogenies.

117

## 118 **2. Geological setting of magmatic events**

119

120 The following description follows a SW-NE palaeogeographic transect throughout the  
121 south-western European margin of Gondwana during Cambro–Ordovician times.

122

### 123 **2.1. Central Iberian and Galicia-Trás-os-Montes Zones**

124

125 In the Ossa Morena and southern Central Iberian Zones of the Iberian Massif (Fig. 1A–  
126 B), the so-called Toledanian Phase is recognized as an angular discordance that  
127 separates variably tilted Ediacaran–Cambrian Series 2 rifting volcanosedimentary  
128 packages from overlying passive-margin successions. The Toledanian gap comprises,  
129 at least, most of the Furongian and basal Ordovician, but the involved erosion can  
130 incise into the entire Cambrian and the upper Ediacaran Cadomian basement  
131 (Gutiérrez-Marco et al., 2019; Álvaro et al., 2019; Sánchez-García et al., 2019).

132 Recently, Sánchez-García et al. (2019) have interpreted the Toledanian Phase as a  
133 break-up (or rift/drift) unconformity with the Armorican Quartzite (including the Purple



134 Series and Los Montes Beds; McDougall et al., 1987; Gutiérrez-Alonso et al., 2007;  
135 Shaw et al., 2012, 2014) sealing an inherited Toledanian palaeorelief (Fig. 2).  
136 The phase of uplift and denudation of an inherited palaeorelief composed of upper  
137 Ediacaran–Cambrian rocks is associated with the massive outpouring of felsic-  
138 dominant calc-alkaline magmatic episodes related to neither metamorphic nor cleavage  
139 features. This magmatic activity is widely distributed throughout several areas of the  
140 Iberian Massif, such as the Cantabrian Zone and the easternmost flank of the West  
141 Asturian-Leonese Zone, where sills and rhyolitic lava flows and volcaniclastics mark  
142 the base of the Armorican Quartzite (dated at  $477.5 \pm 0.9$  Ma; Gutiérrez-Alonso et al.,  
143 2007, 2016), and the lower Tremadocian Borrachón Formation of the Iberian Chains  
144 (Álvaro et al., 2008). Similar ages have been reported in the igneous rocks of the Basal  
145 Allochthonous Units and the Schistose Domain in the Galicia-Trás-os-Montes Zone  
146 (500–462 Ma; Valverde-Vaquero et al., 2005, 2007; Montero et al., 2009; Talavera et  
147 al., 2008, 2013; Dias da Silva et al., 2012, 2014; Díez Fernández et al., 2012; Farias et  
148 al., 2014) and different areas of the Central Iberian Zone, including the contact  
149 between the Central Iberian and Ossa-Morena Zones, where the Carrascal and  
150 Portalegre batoliths are intruded and the felsic volcanosedimentary Urra Formation is  
151 interbedded (494–470 Ma, Solá et al., 2008; Antunes et al., 2009; Neiva et al., 2009;  
152 Romaõ et al., 2010; Rubio-Ordóñez et al., 2012; Villaseca et al., 2013) (Fig. 1B).  
153 The most voluminous Toledanian-related volcanic episode is represented by the  
154 Ollo de Sapo Formation, which covers the northeastern Central Iberian Zone. It mainly  
155 consists of felsic volcanosedimentary and volcanic rocks interbedded at the base of the  
156 Lower Ordovician strata and plutonic bodies. The Ollo de Sapo volcanosedimentary  
157 Formation has long been recognized as an enigmatic Furongian–Early Ordovician  
158 (495–470 Ma) magmatic event exposed along the core of a 600 km-long antiform  
159 (labelled as 77 in Fig. 1B) (Valverde-Vaquero and Dunning, 2000; Bea et al., 2006;  
160 Montero et al., 2007, 2009; Zeck et al., 2007; Castiñeiras et al., 2008a; Díez Montes et  
161 al., 2010; Navidad and Castiñeiras, 2011; Talavera et al., 2013; López-Sánchez et al.,



162 2015; Díaz-Alvarado et al., 2016; Villaseca et al., 2016; García-Arias et al., 2018). The  
163 peak of magmatic activity was reached at ca. 490–485 Ma and its most recognizable  
164 characteristic is the presence of abundant megacrysts of K-feldspar, plagioclase and  
165 blue quartz. There is no evident space-time relationship in its distribution (for a  
166 discussion, see López-Sánchez et al., 2015) and, collectively, the Ollo de Sapo  
167 Formation rocks constitute a major tectonothermal event whose expression can be  
168 found in most of the Variscan massifs of continental Europe including the Armorican  
169 and Bohemian massifs (e.g., von Quadt, 1997; Kröner and Willmer, 1998; Linnemann  
170 et al., 2000; Tichomirowa et al., 2001; Friedl et al., 2004; Mingram et al., 2004; Teipel  
171 et al., 2004; Ballèvre et al., 2012; El Korrh et al., 2012; Tichomirowa et al., 2012; for a  
172 summary, see Casas and Murphy, 2018). The large amount of magmatic rocks located  
173 in the European Variscan Belt led some authors to propose the existence of a siliceous  
174 Large Igneous Province (LIP) (Díez Montes et al., 2010; Gutiérrez-Alonso et al., 2016),  
175 named Ibero-Armorican LIP by García-Arias et al. (2018).

176

## 177 **2.2. Eastern Pyrenees**

178

179 In the eastern Pyrenees, earliest Ordovician volcanic-free passive-margin conditions,  
180 represented by the Jujols Group (Padel et al., 2018), were followed by a late Early–Mid  
181 Ordovician phase of uplift and erosion that led to the onset of the Sardic unconformity  
182 (Fig. 2). Uplift was associated with magmatic activity, which pursued until Late  
183 Ordovician times. An extensional pulsation took place then developing normal faults  
184 that controlled the sedimentation of post–Sardic siliciclastic deposits infilling  
185 palaeorelief depressions. Acritarchs recovered in the uppermost part of the Jujols  
186 Group suggest a broad Furongian–earliest Ordovician age (Casas and Palacios, 2012),  
187 conterminous with a maximum depositional age of ca. 475 Ma, based on the age of the  
188 youngest detrital zircon populations (Margalef et al., 2016). On the other hand, a ca.  
189 459 Ma U–Pb age for the Upper Ordovician volcanic rocks overlying the Sardic



190 Unconformity has been proposed in the eastern Pyrenees (Martí et al., 2019), and ca.  
191 455 and 452 Ma in the neighbouring Catalan Coastal Ranges, which represents the  
192 southern prolongation of the Pyrenees (Navidad et al., 2010; Martínez et al., 2011).  
193 Thus, a time gap of about 16–23 m.y. can be related to the Sardic Phase in the eastern  
194 Pyrenees and the neighbouring Catalan Coastal Ranges.

195 Coeval with the late Early–Mid Ordovician phase of generalized uplift and  
196 denudation, a key magmatic activity led to the intrusion of voluminous granitoids, about  
197 500 to 3000 m thick and encased in strata of the Ediacaran–Lower Ordovician  
198 Canaveilles and Jujols groups (Fig. 2). These granitoids constitute the protoliths of the  
199 large orthogneissic laccoliths that punctuate the backbone of the eastern Pyrenees.  
200 These are, from west to east (Fig. 1D), the Aston ( $470 \pm 6$  Ma, Denèl et al., 2009;  $467$   
201  $\pm 2$  Ma, Mezger and Gerdes, 2016), Hospitalet ( $472 \pm 2$  Ma, Denèl et al., 2009),  
202 Canigó ( $472 \pm 6$  Ma, Cocherie et al., 2005;  $462 \pm 1.6$  Ma, Navidad et al., 2018), Roc de  
203 Frausa ( $477 \pm 4$  Ma, Cocherie et al., 2005;  $476 \pm 5$  Ma, Castiñeiras et al., 2008b) and  
204 Albera ( $470 \pm 3$  Ma, Liesa et al., 2011) massifs, which comprise a dominant Floian–  
205 Dapingian age. It is noticeable the fact that only a minor representation of coeval basic  
206 magmatic rocks are outcropped. The acidic volcanic equivalents have been  
207 documented in the Albera massif, where subvolcanic rhyolitic porphyroid rocks have  
208 yielded similar ages to those of the main gneissic bodies at  $465 \pm 4$ ,  $472 \pm 3$ ,  $473 \pm 2$   
209 and  $474 \pm 3$  Ma (Liesa et al., 2011). Similar acidic byproducts are represented by the  
210 rhyolitic sills of Pierrefite (Calvet et al., 1988).

211 The late Early–Mid Ordovician (“Sardic”) phase of uplift was succeeded by a Late  
212 Ordovician extensional pulsation responsible for the opening of (half-)grabens infilled  
213 with the basal Upper Ordovician alluvial-to-fluvial conglomerates (La Rabassa  
214 Formation). At cartographic scale, a set of NE-SW trending normal faults abruptly  
215 disturbing the thickness of the basal Upper Ordovician formations can be recognized in  
216 the La Cerdanya area (Casas and Fernández, 2007; Casas, 2010). Sharp variations in  
217 the thickness of the Upper Ordovician strata have been documented by Hartevelt



218 (1970) and Casas and Fernández (2007). Drastic variations in grain size and thickness  
219 can be attributed to the development of palaeotopographies controlled by faults and  
220 subsequent erosion of uplifted palaeoreliefes, with subsequent infill of depressed areas  
221 by alluvial fan and fluvial deposition, finally sealed by Silurian sediments (Puddu et al.,  
222 2019). A Late Ordovician magmatic pulsation contemporaneously yielded a varied set  
223 of magmatic rocks. Small granitic bodies are encased in the Canaveilles and Jujols  
224 strata of the Canigó massif. They constitute the protoliths of the Cadí ( $456 \pm 5$  Ma,  
225 Casas et al., 2010), Casemí ( $446 \pm 5$  and  $452 \pm 5$  Ma, Casas et al., 2010), Núria ( $457 \pm$   
226  $4$  and  $457 \pm 5$  Ma, Martínez et al., 2011) and Canigó G-1 type ( $457 \pm 1.6$  Ma, Navidad  
227 et al., 2018) gneisses.

228 The lowermost part of the Canaveilles Group (the so-called Balaig Series) host  
229 metre-scale thick bodies of metadiorite interbeds related to an Upper Ordovician  
230 protolith, ( $453 \pm 4$  Ma, SHRIMP U–Pb in zircon, Casas et al., 2010). Coeval calc-  
231 alkaline ignimbrites, andesites and volcaniclastic rocks are interbedded in the Upper  
232 Ordovician succession of the Bruguera and Ribes de Freser areas (Robert and  
233 Thiebaut, 1976; Ayora, 1980; Robert, 1980; Martí et al., 1986, 2019). In the Ribes area,  
234 a granitic body with granophyric texture, dated at  $458 \pm 3$  Ma by Martínez et al. (2011),  
235 intruded at the base of the Upper Ordovician succession. In the La Pallaresa dome,  
236 some metre-scale rhyodacitic to dacitic subvolcanic sills, Late Ordovician in age (ca.  
237 453 Ma, Clariana et al., 2018), occur interbedded within the pre-unconformity strata  
238 and close to the base of the Upper Ordovician.

239

### 240 **2.3. Occitan Domain: Albigeois, Montagne Noire and Mounhoumet massifs**

241

242 The parautochthonous framework of the southern French Massif Central, named  
243 Occitan Domain by Pouclet et al., (2017), includes among others, from south to north,  
244 the Mounhoumet, Montagne Noire and Albigeois massifs. The domain represents an  
245 eastern prolongation of the Variscan South Armorican Zone (including southwestern



246 Bretagne and Vendée). Since Gèze (1949) and Arthaud (1970), the southern edge of  
247 the French Massif Central has been traditionally subdivided, from north to south, into  
248 the northern, axial and southern Montagne Noire (Fig. 1C). The Palaeozoic succession  
249 of the northern and southern sides includes sediments ranging from late Ediacaran to  
250 Silurian and from Terreneuvian (Cambrian) to Visean in age, respectively. These  
251 successions are affected by large scale, south-verging recumbent folds that display a  
252 low to moderate metamorphic grade. Their emplacement took place in Late Visean to  
253 Namurian times (Engel et al., 1980; Feist and Galtier, 1985; Echtler and Malavieille,  
254 1990). The Axial Zone consists of plutonic, migmatitic and metamorphic rocks globally  
255 arranged in a bulk dome oriented ENE-WSW (Fig. 1C), where four principal lithological  
256 units can be recognized (i) schists and micaschists, (ii) migmatitic orthogneisses, (iii)  
257 metapelitic metatexites, and (iv) diatexites and granites (Cocherie, 2003; Faure et al.,  
258 2004; Roger et al., 2004, 2015; Bé Mézème, 2005; Charles et al., 2009; Rabin et al.,  
259 2015). The Rosis micaschist synform subdivides the eastern Axial Zone into the  
260 Espinouse and Caroux sub-domes, whereas the southwestern edge of the Axial Zone  
261 comprises the Nore massif.

262 In the Occitan Domain, two main Cambro–Ordovician felsic events can be identified  
263 giving rise to the protoliths of (i) the Larroque metarhyolites in the northern Montagne  
264 Noire and Albigeois, thrusted from Rouergue; and (ii) the migmatitic ortogneisses in the  
265 Axial Zone of the Montagne Noire (Fig. 2).

266 (i) The Larroque volcanosedimentary Complex is a thick (500–1000 m) package of  
267 porphyroclastic metarhyolites located on the northern Montagne Noire (Lacaune  
268 Mountains), Albigeois (St-Salvi-de-Carcavès and St-Sernin-sur-Rance nappes) and  
269 Rouergue; the Variscan setting of the formation is allochthonous in the Albigeois and  
270 parautochthonous in the rest. This volcanism emplaced above the Furongian strata and  
271 the so-called “Série schisto-gréseuse verte” (see Guérangé-Lozes et al., 1996;  
272 Guérangé-Lozes and Alabouvette, 1999), and is encased in the upper part of the  
273 Miaolingian La Gardie Formation (Pouclet et al., 2017) (Fig. 2). The Larroque volcanic



274 rocks consist of deformed microgranites or porphyroclastic rhyolites rich in largely  
275 fragmented, lacunous (rhyolitic) quartz and alkali feldspar phenocrysts. The  
276 metarhyolites occur as porphyritic lava flows, sills and other associated facies, such as  
277 aphyric lava flows, porphyritic and aphyric pyroclastic flows of welded or unwelded  
278 ignimbritic types, fine to coarse tephra deposits, and epiclastic and volcaniclastic  
279 deposits. Although these rocks are also named “augen gneiss”, they do not display a  
280 high-grade gneiss paragenesis but a general lower grade metamorphic mineralogy.  
281 The Occitan augen gneisses mimic the “Ollo de Sapo” facies from the Central Iberian  
282 Zone because of their large bluish quartz phenocrysts. Based on geochemical  
283 similarities and contemporaneous emplacement, Pouclet et al. (2017) suggested that  
284 this event also supplied the Davejean acidic volcanic rocks in the Mouthoumet Massif,  
285 which represent the southern prolongation of the southern Montagne Noire (Fig. 2),  
286 and the Génis rhyolitic unit of the western Limousin sector.

287 (ii) Some migmatitic orthogneisses make up the southern Axial Zone, from the  
288 western Cabardès to the eastern Caroux domes. The orthogneisses, derived from  
289 Ordovician metagranites bearing large K-feldspar phenocrysts, were emplaced at 471  
290  $\pm 4$  Ma (Somail Orthogneiss, Cocherie et al., 2005), 456  $\pm 3$  and 450  $\pm 6$  Ma (Pont de  
291 Larn and Gorges d'Héric gneisses, Roger et al., 2004) and 455  $\pm 2$  Ma (Sain Europe  
292 gneiss, Pitra et al., 2012). They intruded a metasedimentary pile, traditionally known as  
293 “Schistes X” and formally named St. Pons-Cabardès Group (Fig. 2). The latter consists  
294 of schists, greywackes, quartzites and subsidiary volcanic tuffs and marbles (Demange  
295 et al., 1996; Demange, 1999; Alabouvette et al., 2003; Roger et al., 2004; Cocherie et  
296 al., 2005). The group is topped by the Sériès Tuff, dated at 545  $\pm 15$  Ma (Lescuyer and  
297 Cocherie, 1992), which represents a contemporaneous equivalent of the Cadomian  
298 Riverous rhyolitic tuff (542.5  $\pm 1$  and 537.1  $\pm 2.5$  Ma) from the Lodève inlier of the  
299 northern Montagne Noire (Álvaro et al., 2014b, 2018; Padel et al., 2017). Migmatization  
300 has been dated by monacites from migmatites and anatetic granites at 327  $\pm 7$ , 333  $\pm$



301 6 and  $333 \pm 4$  Ma (Bé Mézème, 2005; Charles et al., 2008); as a result, the 330–325  
302 Ma time interval can represent a Variscan crustal melting event in the Axial Zone.  
303 As in the Pyrenees, the Middle Ordovician is absent in the Occitan Domain. Its gap  
304 allows distinction between a Lower Ordovician pre-unconformity sedimentary package  
305 para- to unconformably overlain by an Upper Ordovician–Silurian succession (Álvaro et  
306 al., 2016; Pouplet et al., 2017).

307

308 **2.4. Sardinia**

309

310 In Sardinia the Cambro–Ordovician magmatism is well represented in the external  
311 (southern) and internal (northern) nappe zones of the exposed Variscan Belt (Fig. 1E),  
312 and ranges in age from late Furongian to Late Ordovician. A Furongian–Tremadocian  
313 (ca. 491–480 Ma) magmatic activity, predating the Sardic phase, is mostly represented  
314 by felsic volcanic and subvolcanic rocks encased in the San Vito sandstone Formation.  
315 The Sardic-related volcanic products differ from one nappe to another: intermediate  
316 and basic (mostly metandesites and andesitic basalts) are common in the nappe  
317 stacking of the central part of the island (Barbagia and Goceano), whereas felsic  
318 metavolcanites prevail in the southeastern units. Their age is bracketed between 465  
319 and 455 Ma (Giacomini et al., 2006; Oggiano et al., 2010; Pavanetto et al., 2012;  
320 Cruciani et al., 2018) and matches the Sardic gap based on biostratigraphy (Barca et  
321 al., 1988).

322 Teichmüller (1931) and Stille (1939) were the first to recognize in southwestern  
323 Sardinia an intra–Ordovician stratigraphic hiatus. Its linked erosive unconformity is  
324 supported by a correlatable strong angular discordance in the Palaeozoic basement of  
325 the Iglesiente-Sulcis area, External Zone (Carmignani et al., 2001). This major  
326 discontinuity separates the Cambrian–Lower Ordovician Nebida, Gonnese and Iglesias  
327 groups (Pillola et al., 1998) from the overlying coarse-grained (“Puddinga”) Monte  
328 Argentu metasediments (Leone et al., 1991, 2002; Laske et al., 1994). The gap



329 comprises a chronostratigraphically constrained minimum gap of about 18 m.y. that  
330 includes the Floian and Dapingian (Barca et al., 1987, 1988; Pillola et al., 1998; Barca  
331 and Cherchi, 2004) (Fig. 2). The hiatus is related to neither metamorphism nor  
332 cleavage, though some E-W folds have been documented in the Gonnesa Anticline  
333 and the Iglesias Syncline (Cocco et al., 2018), which are overstepped by the  
334 “Puddinga” metaconglomerates. Both the E-W folds and the overlying  
335 metaconglomerates were subsequently affected by Variscan N-S folds (Cocco and  
336 Funneda, 2011, 2017). Sardic-related volcanic rocks are not involved in this area, but  
337 Sardic-inherited palaeoreliefes are lined with breccia slides that include metre- to  
338 decametre-scale carbonate boulders (“Olistoliti”), some of them hosting  
339 synsedimentary faults contemporaneously mineralized with ore bodies (Boni and  
340 Koeppel, 1985; Boni, 1986; Barca, 1991; Caron et al., 1997). The lower part of the  
341 unconformably overlying Monte Argentu Formation deposited in alluvial to fluvial  
342 environments (Martini et al., 1991; Loi et al., 1992; Loi and Dabard, 1997).

343 A similar gap was reported by Calvino (1972) in the Sarrabus-Gerrei units of the  
344 External Nappe Zone. The so-called “Sarrabese Phase” is related to the onset of thick,  
345 up to 500 m thick, volcanosedimentary complexes and volcanites (Barca et al., 1986;  
346 Di Pisa et al., 1992) with a Darriwilian age for the protoliths of the metavolcanic rocks  
347 (464 ± 1 Ma, Giacomini et al., 2006; 465.4 ± 1.9 Ma, Oggiano et al., 2010). In the  
348 Iglesiente-Sulcis region (Fig. 1E), Carmignani et al. (1986, 1992, 1994, 2001)  
349 suggested that the “Sardic-Sarrabese phase” should be associated with the  
350 compression of a Cambro-Ordovician back-arc basin that originated the migration of  
351 the Ordovician volcanic arc toward the Gondwanan margin.

352 Some gneissic bodies, interpreted as the plutonic counterpart of metavolcanic rocks,  
353 are located in the Bithia unit (Monte Filau areas, 457.5 ± 0.33 and 458.21 ± 0.32 Ma,  
354 Pavanello et al., 2012) and in the internal units (Lodè orthogneiss, 456 ± 14 Ma;  
355 Tanaunella orthogneiss, 458 ± 7 Ma, Helbing and Tiepolo, 2005; Golfo Aranci  
356 orthogneiss, 469 ± 3.7 Ma, Giacomini et al., 2006).



357        The Sardic palaeorelief is sealed by Upper Ordovician transgressive deposits. The  
358        sedimentary facies show high variability, but the –mostly terrigenous– sediments vary  
359        from grey fine- to medium-sized sandstones, to muddy sandstones and mudstones.  
360        They are referred to the Katian Punta Serpeddi and Orroeledu formations (Pistis et al.,  
361        2016). This post-Sardic sedimentary succession is coeval with a new magmatic  
362        pulsation represented by alkaline to tholeiitic within-plate basalts (Di Pisa et al., 1992;  
363        Gaggero et al., 2012).

364

### 365        **3. Geochemical data**

366

367        The rocks selected for geochemical analysis (231 samples; geographically settled in  
368        Fig. 1 and stratigraphically in Fig. 2) have recorded different degrees of  
369        hydrothermalism and metamorphism, as a result of which only the most immobiles  
370        elements have been considered. The geochemical calculations, in which the major  
371        elements take part, have been made from values recalculated to 100 in volatile free  
372        compositions; Fe is reported as FeO<sub>t</sub>.

373        The geochemical dataset of the Central Iberian Zone includes 152 published  
374        geochemical data, from which 85 are plutonic and 67 volcanic and volcaniclastic rocks  
375        from the Ollo de Sapo Formation (Galicia, Sanabria and Guadarrama areas), and the  
376        contact between the Central Iberian and Ossa Morena Zones (Urra Formation and  
377        Portalegre and Carrascal granites). Other data were yielded from six volcanic rocks of  
378        the Galicia-Trás-os-Montes Zone (Saldanha area) (Fig. 1B; Repository Data).

379        The dataset of the eastern Pyrenees consists of 38 samples, six of which are upper  
380        Lower Ordovician volcanic rocks, and seven upper Lower Ordovician plutonic rocks,  
381        together with nine Upper Ordovician volcanic and 14 Upper Ordovician plutonic rocks  
382        (Repository Data). New data reported below include two samples of subvolcanic sills  
383        intercalated in the pre-Sardic unconformity succession (Clariana et al., 2018; Margalef,  
384        unpubl.; Table 1).



385        The study samples from the Occitan Domain comprise six metavolcanites, four from  
386        the Larroque volcanosedimentary Complex in the Albigeois and northern Montagne  
387        Noire and two from the Mounhoumet massif (Pouclet et al., 2017) (Repository Data),  
388        and four new samples for the Axial Zone gneisses (Table 1).

389        In the Sardinian dataset, 25 published analyses are selected: five correspond to the  
390        Golfo Aranci orthogneiss (Giacomini et al., 2006), six to metavolcanites from the central  
391        part of the island (Giacomini et al., 2006; Cruciani et al., 2013), and five to  
392        metavolcanites and one to gneisses from the Bithia unit (Cruciani et al., 2018)  
393        (Repository Data). Ten new analyses are added from the Monte Filau and Capo  
394        Spartivento gneisses of the Bithia unit, and from the Punta Bianca gneisses embedded  
395        within the migmatites of the High-grade Metamorphic complex of the Inner Zone (Table  
396        1).

397        A general classification of these samples, following Winchester and Floyd (1977),  
398        can be seen in Figure 3A–B, and the geographical coordinates of the new samples in  
399        Table 1. For geochemical comparison (Table 2), two large groups or suites are  
400        differentiated in order to check the similarities and differences between the magmatic  
401        rocks, and to infer a possible geochemical trend following a palaeogeographic SW-to-  
402        NE transect. The description reported below follows the same palaeogeographic and  
403        chronological order.

404

### 405        **3.1. Furongian-to-Mid Ordovician Suite**

406

407        In the Central Iberian and Galicia-Trás-os-Montes Zones, the Furongian-to-Mid  
408        Ordovician magmatic activity is pervasive. Their main representative is the Ollo de  
409        Sapo Formation, which includes volcanic and subvolcanic rocks (67 samples) as well  
410        as plutonic rocks (85 samples) (data from Murphy et al., 2006; Díez-Montes, 2007;  
411        Montero et al., 2007, 2009; Solá, 2007; Solá et al., 2008; Talavera, 2009; Villaseca et  
412        al., 2016). From the Parautochthon Schistose Domain of the Galicia-Trás-os Montes



413 Zone, six samples of rhyolite tuffs of the Saldanha Formation (Dias da Silva et al.,  
414 2014) are selected, which share geochemical features with the Ollo de Sapo  
415 Formation.

416 (i) The composition of the Ollo de Sapo-facies orthogneisses (OG in the figures)  
417 ranges from potassium-rich dacite to rhyolite ( $60.3 < \text{SiO}_2 < 75$  wt. %;  $0.1 < \text{Na}_2\text{O} < 3.9$   
418 wt. %;  $3.4 < \text{K}_2\text{O} < 5.9$  wt. %; Figs. 3–4). This subgroup, with peraluminous A/CNK ratio  
419 (3.1–1.0), includes samples of the Ollo de Sapo Formation from the Sanabria and  
420 Guadarrama areas, the former dated at  $472 \pm 1$  Ma (Díez-Montes, 2007) and the latter  
421 between  $488 \pm 3$  and  $473 \pm 8$  Ma (Valverde-Vaquero and Dunning, 2000; Navidad and  
422 Castiñeiras, 2011; Talavera et al., 2013; Villaseca et al., 2016).  $\varepsilon\text{Nd}$  values range from  
423 –1.8 to –5.1, and  $T_{\text{DM}}$  from 1.8 to 1.1 Ga (Montero et al., 2007, 2009; Villaseca et al.,  
424 2016).

425 (ii) The composition of the leucogneisses (LG) ranges from potassium-rich dacite to  
426 rhyolite ( $73.6 < \text{SiO}_2 < 75.9$  wt. %;  $2.7 < \text{Na}_2\text{O} < 3.1$  wt. %;  $4.2 < \text{K}_2\text{O} < 5.3$  wt. %; Figs.  
427 3–4). The A/CNK ratio is peraluminous (1.1–1.3). This subgroup includes samples from  
428 the Guadarrama region.  $\varepsilon\text{Nd}$  values range from –4.9 to –5.1, and  $T_{\text{DM}}$  is 4.1 Ga  
429 (Villaseca et al., 2016). These samples display erroneous  $T_{\text{DM}}$  values in two of the three  
430 considered samples, with high  $^{147}\text{Sm}/^{144}\text{Nd}$  ratios ( $> 0.13$ ), a character relatively  
431 common in felsic rocks (DePaolo, 1988; Martínez et al., 2011).

432 (iii) The composition of the granites (GRA) ranges from potassium-rich dacite to  
433 rhyolite ( $64.6 < \text{SiO}_2 < 77$  wt. %;  $0.5 < \text{Na}_2\text{O} < 4.8$  wt. %;  $2.5 < \text{K}_2\text{O} < 6.3$  wt. %; Figs.  
434 3–4). The A/CNK ratio is peraluminous (1.8–1.0). This subgroup includes samples from  
435 the northeastern Central System, Sanabria, Miranda do Douro and the western Central  
436 Iberian Zone. The age of the involved metagranites is  $487 \pm 4$  Ma (Montero et al.,  
437 2009) and  $488 \pm 6$  Ma (Díez Montes, 2007);  $473 \pm 3$  Ma (Talavera, 2009) and  $496 \pm 2$   
438 Ma (Zeck et al., 2007) for the Miranda do Douro metagranites;  $489 \pm 5$  Ma for the  
439 Vitigudino metagranites;  $486 \pm 6$  for the Fermoselle metagranites; and  $471 \pm 7$  Ma for  
440 the Ledesma metagranite (Talavera, 2009). In the southern Central Iberian Zone, the



441 Carrascal metagranite has been dated between 479 to 486 Ma (Solá, 2007) and the  
442 Portalegre metagranite between  $482 \pm 4$  and  $492 \pm 3$  Ma (Solá, 2007).  $\varepsilon_{\text{Nd}}$  values  
443 range from +2.6 to -5.2, and  $T_{\text{DM}}$  from 0.90 to 3.6 Ga (Montero et al., 2007; Solá, 2007;  
444 Talavera, 2009).

445 (iv) The composition of the volcanic rocks (VOL) ranges from andesite to rhyolite  
446 ( $64.6 < \text{SiO}_2 < 79.3$  wt. %;  $0.1 < \text{Na}_2\text{O} < 3.2$  wt. %;  $2.2 < \text{K}_2\text{O} < 6.3$  wt. %; Figs. 3–4).

447 The A/CNK ratio is peraluminous (2.7–1.1). This subgroup includes samples from the  
448 Saldanha Formation in the Galicia-Trás-os-Montes Zone, the metavolcanic rocks of the  
449 Ollo de Sapo Formation in the Sanabria region and the Urra Formation.  $\varepsilon_{\text{Nd}}$  values  
450 range from -1.6 to -5.5, and  $T_{\text{DM}}$  from 1.7 to 1.3 Ga (Montero et al., 2007; Solá, 2007).

451 (v) The composition of the San Sebastián orthogneisses (OSS) is rhyolitic ( $73.8 <$   
452  $\text{SiO}_2 < 75.4$  wt. %;  $2.5 < \text{Na}_2\text{O} < 3.1$  wt. %;  $4.9 < \text{K}_2\text{O} < 5.4$  wt. %; Figs. 3–4). The  
453 A/CNK ratio is peraluminous (1.2–1.1). The San Sebastián orthogneisses are located  
454 in the Sanabria region, on the northern Central Iberian Zone, and are dated at  $465 \pm 10$   
455 Ma (Lancelot et al., 1985) and 470 Ma (Talavera, 2009). They display weakly positive  
456  $\varepsilon_{\text{Nd}}$  values (-0.0 to -4.0), and  $T_{\text{DM}}$  from 1.6 to 1.2 Ga (Talavera, 2009). This subgroup  
457 is mainly characterized by its alkaline character.

458 In the eastern Pyrenees, an Early–Mid Ordovician magmatic activity gave rise to the  
459 intrusion of voluminous (about 500–3000 m in size) aluminous granitic bodies, encased  
460 into the Canaveilles and Jujols beds (Álvaro et al., 2018; Casas et al., 2019). They  
461 constitute the protoliths of the large orthogneissic laccoliths that form the core of the  
462 domal massifs scattered throughout the backbone of the Pyrenees. Rocks of the  
463 Canigó, Roc de Frausa and Albera massifs have been taken into account in this work,  
464 in which volcanic rocks of the Pierrefite and Albera massifs, and the so-called G3  
465 orthogneisses by Guitard (1970) are also included. All subgroups vary compositionally  
466 from subalkaline andesite to rhyolite, as illustrated in the Pearce's (1996) diagram of  
467 Figure 4 (data compiled from Vilà et al., 2005; Castiñeiras et al., 2008b; Liesa et al.,  
468 2011; Navidad et al., 2018).



469        Although most rocks in this area are acidic, it is remarkable the presence of minor  
470        mafic bodies (Cortalet and Marialles metabasites, not studied in this work), which could  
471        indicate a mantellic connection with parental magmas during the Mid and Late  
472        Ordovician. As well, it should be noted that there are no andesitic rocks in the area.

473        (vi) The composition of the ocelar orthogneisses (G2 *sensu* Guitard, 1970) ranges  
474        from dacite to rhyolite ( $68.3 < \text{SiO}_2 < 73.6$  wt. %;  $3.2 < \text{Na}_2\text{O} < 3.9$  wt. %;  $2.5 < \text{K}_2\text{O} < 4.4$   
475        wt. %; Fig. 4). The age of this subgroup, with a peraluminous A/CNK ratio (1.2–1.1),  
476        ranges from 476 to 462 Ma,  $\varepsilon\text{Nd}$  values from –4.4 to –3.0, and  $T_{\text{DM}}$  from 1.20 to 1.44  
477        Ga (Vilà et al., 2005; Castiñeiras et al., 2008b; Liesa et al., 2011; Navidad et al., 2018).

478        (vii) The composition of the G3 orthogneisses correspond to a potassium-rich dacite  
479        ( $68.4 < \text{SiO}_2 < 73.5$  wt. %;  $2.4 < \text{Na}_2\text{O} = 2.9$  wt. %;  $\text{K}_2\text{O} = 4.4$  wt. %; Fig. 4). The A/CNK  
480        ratio is peraluminous (1.2). These rocks are dated at  $463 \pm 1$  Ma (Navidad et al., 2018).

481         $\varepsilon\text{Nd}$  value is –4.2 and  $T_{\text{DM}}$  is 1.33 Ga (Navidad et al., 2018).

482        (viii) The composition of the volcanic rocks (V1) is of a sodium-rich rhyolite ( $68.4 <$   
483         $\text{SiO}_2 < 73.5$  wt. %;  $2.4 < \text{Na}_2\text{O} < 7.88$  wt. %;  $1.27 < \text{K}_2\text{O} < 3.2$  wt. %; Fig. 4). The  
484        A/CNK ratio is peraluminous (2.0–1.1) (Calvet et al., 1988; Liesa et al., 2011). This  
485        subgroup includes samples from the Pierrefite Formation and the Albera massif. The  
486        latter has been dated from  $465 \pm 4$  to  $472 \pm 3$  Ma (Liesa et al., 2011).  $\varepsilon\text{Nd}$  value ranges  
487        between –5.1 and –2.6, and TDM between 1.6 and 1.7 Ga (Liesa et al., 2011;  
488        unpublised data).

489        In the Occitan Domain, six samples of the Larroque volcanosedimentary Complex  
490        (Early Tremadocian in age) consist of basin floors and subaerial explosive and effusive  
491        rhyolites (Pouclet et al., 2017). The porphyroclastic rocks of the Larroque metarhyolites  
492        were sampled in the Saint-Géraud and Larroque areas from the Saint-Sernin-sur-  
493        Rance nappe and the Saint-André klippe above the Saint-Salvi-de-Carcavès nappe  
494        (Pouclet et al., 2017).



495 (ix) The composition of the Occitan volcanic rocks (VOL-OD) ranges from  
496 potassium-rich dacite to rhyolite ( $66.7 < \text{SiO}_2 < 75.6$  wt. %;  $0.6 < \text{Na}_2\text{O} < 3.7$  wt. %;  $2.3 < \text{K}_2\text{O} < 9.3$  wt. %; Fig. 4). The A/CNK ratio is peraluminous (2.4–1.3).

498 In the Middle Ordovician rocks of Sardinia, 11 samples are selected, five of which  
499 correspond to orthogneisses of the Aranci Gulf, in the Inner Zone of the NE island  
500 (Giacomini et al., 2006), completed with six volcanic rocks of the External Zone  
501 (Giacomini et al., 2006; Cruciani et al., 2018).

502 (x) The composition of the Sardinian orthogneisses (OG-SMO) corresponds to a  
503 potassium-rich rhyolite ( $74 < \text{SiO}_2 < 67.2$  wt. %;  $2.6 < \text{Na}_2\text{O} < 3.8$  wt. %;  $2.3 < \text{K}_2\text{O} < 5.8$   
504 wt. %; Fig. 4). These rocks, with a peraluminous A/CNK ratio (1.26–1.11), have been  
505 dated at  $469 \pm 1$  Ma (Giacomini et al., 2006).

506 (xi) Finally, the composition of the Sardinian volcanic rocks (VOL-SMO) ranges  
507 from potassium-rich dacite to rhyolite ( $67.6 < \text{SiO}_2 < 76.7$  wt. %;  $1.9 < \text{Na}_2\text{O} < 4.7$  wt.  
508 %;  $2.9 < \text{K}_2\text{O} < 5.4$  wt. %; Fig. 4). The age of these rocks vary between  $464 \pm 1$  Ma  
509 (Giacomini et al., 2006) and  $462 \pm 4.3$  Ma (Cruciani et al., 2018). The A/CNK ratio is  
510 peraluminous (2.02–1.22).

511

### 512 3.2 Upper Ordovician Suite

513

514 In the eastern Pyrenees, four Upper Ordovician subgroups are distinguished based on  
515 their field occurrence and geochemical and geochronological features: the G1-type  
516 orthogneisses *sensu* Guitard (1970); the Cadí and Casemí orthogneisses and the  
517 metavolcanic rocks that include the Ribes de Freser rhyolites; the Els Metges volcanic  
518 tuffs; and the rhyolites from Andorra and Pallaresa areas. Clariana et al. (2018) have  
519 dated the latter rhyolites at  $453.6 \pm 1.5$  Ma.

520 (i) The composition of the G1-type orthogneisses ranges from potassium-rich dacite  
521 to rhyodacite ( $73.45 < \text{SiO}_2 < 76.42$  wt. %;  $2.64 < \text{Na}_2\text{O} < 3.13$  wt. %;  $4.73 < \text{K}_2\text{O} < 5.27$   
522 wt. %; Fig. 4). The A/CNK ratio is peraluminous (1.24–1.16). These rocks have been



523 dated at  $457 \pm 1$  Ma (Navidad et al., 2018).  $\varepsilon_{\text{Nd}}$  value ranges between  $-5.3$  and  $-3.1$ ,  
524 and  $T_{\text{DM}}$  between  $1.47$  and  $2.72$  Ga (Martínez et al., 2011; Navidad et al., 2018).

525 (ii) The *CAD*/ orthogneisses show a potassium-rich dacite to rhyodacite  
526 composition ( $\text{SiO}_2 = 69.38$  wt. %;  $\text{Na}_2\text{O} = 3.03$  wt. %;  $\text{K}_2\text{O} = 4.05$  wt. %; Fig. 4). The  
527 A/CNK ratio is peraluminous (1.19). The age of this subgroup is  $456.1 \pm 4.8$  Ma (Casas  
528 et al., 2010).  $\varepsilon_{\text{Nd}}$  value is  $-4.1$  and  $T_{\text{DM}}$  is  $1.47$  Ga (Navidad et al., 2010).

529 (iii) The composition of the *CASEMI*/ orthogneisses ranges from potassium-rich  
530 dacite/rhyodacite to rhyolite ( $71.87 < \text{SiO}_2 < 76.03$  wt. %;  $1.82 < \text{Na}_2\text{O} < 4.02$  wt. %;  
531  $3.24 < \text{K}_2\text{O} < 6.30$  wt. %) (Fig. 4). The A/CNK ratio is peraluminous (1.24–0.94). The  
532 age ranges between  $451.6 \pm 4.8$  Ma and  $445.9 \pm 4.8$  Ma (Casas et al., 2010).  $\varepsilon_{\text{Nd}}$  value  
533 ranges between  $-3.6$  and  $-1.3$ , and  $T_{\text{DM}}$  between  $1.27$  and  $2.63$  Ga (Navidad et al.,  
534 2010).

535 (iv) The composition of the Pyrenean volcanic rocks (V2) is the most variable,  
536 ranging from andesite to dacite/rhyodacite ( $62.98 < \text{SiO}_2 < 86.06$  wt. %;  $0.05 < \text{Na}_2\text{O} <$   
537  $5.98$  wt. %;  $0.63 < \text{K}_2\text{O} < 4.33$  wt. %; Fig. 4). The A/CNK ratio is peraluminous (3.63–  
538 1.04). This subgroup includes the metarhyolites of Ribes de Freser, Andorra (dated at  
539  $457 \pm 1.5$  Ma), Pallaresa ( $453.6 \pm 1.5$  Ma) and Els Metges ( $455.2 \pm 1.8$  Ma, Navidad et  
540 al., 2010).  $\varepsilon_{\text{Nd}}$  ranges between  $-5.1$  and  $-2.6$ , and  $T_{\text{DM}}$  between  $1.62$  and  $1.71$  Ga  
541 (Navidad et al., 2010; Martínez et al., 2011).

542 (v) In the Occitan Domain, four new samples (OG-OD) of orthogneisses from  
543 Gorges d' Heric (Caroux massif), S of Mazamet (Nore massif), S of Rouairoux (Agout  
544 massif) and Le Vintrou are analyzed. The composition of the orthogneisses (OG-OD)  
545 ranges from potassium-rich dacite to rhyolite ( $67.4 < \text{SiO}_2 < 73.9$  wt. %;  $2.8 < \text{Na}_2\text{O} <$   
546  $3.3$  wt. %;  $4.0 < \text{K}_2\text{O} < 4.7$  wt. %; Fig. 4). The A/CNK ratio is peraluminous (1.29–1.20).  
547 The orthogneisses of Gorges d' Heric have been dated at  $450 \pm 3$  Ma (Roger et al.,  
548 2004).  $\varepsilon_{\text{Nd}}$  ranges between  $-3.5$  and  $-4.0$ , and TDM between  $1.8$  and  $1.4$  Ga.

549 (vi) Fourteen samples are selected from the Upper Ordovician of Sardinia. Nine of  
550 them correspond to orthogneisses of the External Zone (OG-SUD, eight samples are



551 new data and one taken from Cruciani et al., 2018), and five samples to volcanic rocks  
552 from the Nappe Zone (VOL-SUD) (Cruciani et al., 2018). The composition of the  
553 orthogneisses ranges from potassium-rich dacite/rhyodacite to rhyolite ( $72.1 < \text{SiO}_2 <$   
554 76.6 wt. %;  $1.6 < \text{Na}_2\text{O} < 3.3$  wt. %;  $4.8 < \text{K}_2\text{O} < 7.8$  wt. %; Fig. 4). The A/CNK ratio is  
555 peraluminous (1.1–1.3). This subgroup has been dated at  $464 \pm 1$  Ma (Giacomini et al.,  
556 2006), and includes samples from Capo Spartivento, Cuile Culurgioni, Tuerredda,  
557 Monte Filau and Monte Settiballas.  $\varepsilon_{\text{Nd}}$  value ranges from –1.6 to –3.3, and  $T_{\text{DM}}$  from  
558 1.2 to 4.2 Ga. The composition of the associated volcanic rocks ranges from  
559 potassium-rich dacite to rhyodacite ( $70.7 < \text{SiO}_2 < 76.7$  wt. %;  $1.6 < \text{Na}_2\text{O} < 3.3$  wt. %;  
560  $4.8 < \text{K}_2\text{O} < 7.8$  wt. %; Fig. 4). The A/CNK ratio is peraluminous (1.1–1.3). This  
561 subgroup includes samples of the Truzzulla Formation at Monte Grighini.

562

#### 563 **4. Geochemical framework**

564

565 A geochemical comparison between the Furongian–Ordovician felsic rocks of all the  
566 above-reported groups offers the opportunity to characterize the successive sources of  
567 crustal-derived melts along the south-western European margin of Gondwana.

568 The geochemical features point to a predominance of materials derived from the  
569 melting of metasedimentary rocks, rich in  $\text{SiO}_2$  and  $\text{K}_2\text{O}$  (average  $\text{K}_2\text{O}/\text{Na}_2\text{O} = 2.25$ )  
570 and peraluminous ( $0.4 < C_{\text{norm}} < 4.5$  and  $0.94 < \text{A/CNK} > 3.12$ ), with only three samples  
571 with  $\text{A/CNK} < 1$  (samples 100786 of the Casemí subgroup, and T26 and T27 of the San  
572 Sebastián subgroup).

573 The result of plotting the REE content vs. average values of continental crust  
574 (Rudnick and Gao, 2004; Fig. 5) yields a flat spectra and a base level shared by most  
575 of the considered groups. The total content in REE is moderate to high (average REE =  
576 176 ppm, ranging between 482.2 and 26.0 ppm; Fig. 6), with a maximum in the  
577 subgroup of the Middle Ordovician volcanic rocks from Sardinia (average REE = 335  
578 ppm, VOL-SMO), and with LREE values more fractionated than HREE ones, and



579 negative anomalies of Eu, which would indicate a characteristic process of magmatic  
580 evolution with plagioclase fractionation. These features are common in peraluminous  
581 granitoids.

582 All subgroups display similar chondritic normalized REE patterns (Fig. 6), with an  
583 enrichment in LREE relative to HREE, which should indicate the involvement of crustal  
584 materials in their parental magmas. Nevertheless, some variations can be highlighted,  
585 such as the lesser fractionation in REE content of some subgroups. These are the  
586 leucogneisses from the Iberian massif ( $LG$ ,  $La/Yb_n = 2.01$ ), the Upper Ordovician  
587 orthogneisses from Sardinia ( $OG-SUO$ ,  $La/Yb_n = 2.94$ ), the Casemí orthogneisses  
588 ( $La/Yb_n = 4.42$ ) and the Middle Ordovician volcanic rocks from Sardinia ( $OG-SUO$ ,  
589  $La/Yb_n = 2.94$ ). This may be interpreted as a greater degree of partial fusion in the  
590 origin of their parental magmas (Rollinson, 1993).

591 There are three geochemical groups displaying  $(Gd/Yb)_n$  values  $> 2$ , and  $(La/Yb)_n$   
592 values  $\geq 9$ . These groups are OSS (Central Iberian Zone), VOL-OD (Occitan Domain)  
593 and G1 (Pyrenees), and share higher alkalinity features.

594 Some V1 rocks from the Pyrenees (Pierrefite Formation) show no negative  
595 anomalies in Eu. Their parental magmas could have been derived from deeper origins  
596 and related to residual materials of the lower continental crust, in areas of production of  
597 K-rich granites (Taylor and McLennan, 1989).

598 The spider diagrams (Fig. 7), however, exhibit strong negative anomalies in Nb, Sr  
599 and Ti, which indicate a distinct crustal affiliation (Díez-Montes, 2007). Only the San  
600 Sebastián orthogneisses (OSS) show distinct discrepancies in respect of the remaining  
601 samples from the Ollo de Sapo Formation. They display lower negative anomalies in  
602 Nb and a more alkaline character by comparison with the rest of the Ollo de Sapo  
603 rocks, which point to alkaline affinities and greater negative anomalies in Nb.

604 Despite some small differences in the chemical ranges of some major elements,  
605 most felsic Ordovician rocks from the Iberian massif (Central Iberian and Galicia-Trás-  
606 os Montes Zones), eastern Pyrenees, Occitan Domain and Sardinia share a common



607 chemical pattern. The Lower–Middle Ordovician rocks of the eastern Pyrenees show  
608 less variation in the content of Zr and Nb (Fig. 7B). The volcanic rocks of these groups  
609 show a different REE behaviour, which would indicate different sources. Two groups  
610 are distinguished in Figure 6, one with greater enrichment in REE and negative  
611 anomaly of Eu, and another with lesser content of HREE and without Eu negative  
612 anomalies.

613 Figure 8 illustrates how the average of all the considered groups approximates the  
614 mean values of the Rudnick and Gao's (2003) Upper Continental Crust. In this figure,  
615 small deviations can be observed, some of them toward LCC values and others toward  
616 BCC, indicating variations in their parental magmas but with quite similar spectra.  
617 Overall chondrite-normalized patterns are close to the values that represent the upper  
618 continental crust, with slight enrichments in the Th/Nb, Th/La and Th/Yb ratios.

619 Finally, in the Occitan volcanic rocks (VOL-OD) the rare earth elements are  
620 enriched and fractionated ( $33.2 \text{ ppm} < \text{La} < 45.6 \text{ ppm}$ ;  $11.2 < \text{La/Yb} < 14.5$ ). The upper  
621 continental crust normalized diagram exhibits negative anomalies of Ti, V, Cr, Mn and  
622 Fe associated with oxide fractionation, of Zr and Hf linked to zircon fractionation, and of  
623 Eu related to plagioclase fractionation. The profiles are comparable to the Vendean  
624 Saint-Gilles rhyolitic ones. The Th vs. Rb/Ba features are also similar to those of the  
625 Saint-Gilles rhyolites, and the Iberian Ollo de Sapo and Urra rhyolites (Solá et al.,  
626 2008; Díez Montes et al., 2010).

627

#### 628 **4.1 Inferred tectonic settings**

629

630 In order to clarify the evolution of geotectonic environments, the data have been  
631 represented in different geotectonic diagrams. The  $\text{Zr}/\text{TiO}_2$  ratio (Lentz, 1996; Syme,  
632 1998) is a key index of compositional evolution for intermediate and felsic rocks. In the  
633 Syme diagram (Fig. 9), most rocks from the Central Iberian Zone represent a  
634 characteristic arc association, although there are some contemporaneous samples



635 characterized by extensional-related values ( $Zr/Ti = 0.10$ , LG). The rocks of the  
636 Middle–Ordovician San Sebastián orthogneisses (OSS) show values of  $Zr/Ti = 0.08$ ,  
637 intermediate between extensional and arc conditions. This could be interpreted as a  
638 sharp change in geotectonic conditions toward the Mid Ordovician (Fig. 9A). For a  
639 better comparison, the samples of the San Sebastián orthogneisses (OSS) and the  
640 granites (GRA) have been distinguished with a shaded area in all the diagrams, since  
641 they have slightly different characteristics to the rest of the samples from the Olio de  
642 Sapo group. The samples G1 (Pyrenees) and VOL (Central Iberian Zone) broadly  
643 share similar values, as a result of which, the three latter groups (OSS, G1 and VOL)  
644 arrange following a good correlation line. The same trend seems to be inferred in the  
645 eastern Pyrenees (Fig. 9B), where the Middle Ordovician subgroups display arc  
646 features, but half of the Upper Ordovician subgroups show extensional affinities (G1  
647 and Casemí orthogneisses). In the case of the Occitan orthogneisses (Fig. 9C), they  
648 show arc characters, which contrast with the contemporaneous volcanic rocks  
649 displaying extensional values with  $Zr/Ti = 0.10$ . This disparity between plutonic and  
650 volcanic rocks could be interpreted as different conditions for the origin of these  
651 magmas. In Sardinia (Fig. 9D), the same evolution from arc to extensional conditions is  
652 highlighted for the Upper Ordovician samples, although some Middle Ordovician  
653 volcanic rocks already shared extensional patterns ( $Zr/Ti = 0.09$ ). In summary, there  
654 seems to be a geochemical evolution in the Ordovician magmas grading from arc to  
655 extensional environments.

656 In the Nb–Y tectonic discriminating diagram of Pearce et al. (1984) (Fig. 10), most  
657 samples plot in the volcanic arc-type, though some subgroups project in the whitin-  
658 plate and anomalous ORG. The majority of samples display very similar  $Zr/Nb$  and  
659  $Nb/Y$  ratios, typical of island arc or active continental margin rhyolites (Díez-Montes et  
660 al., 2010). Only some samples plot separately: OSS samples with highest Nb contents  
661 (>20 ppm), and some volcanic rocks of the Occitan Domain (average Nb = 16.87 ppm).  
662 In the eastern Pyrenees, the Middle Ordovician rocks plot in the volcanic arc field,



663 whereas the Upper Ordovician ones point in the ORG type, except the Casemí  
664 samples. This progress of magmatic sources agrees with the evolution seen in Figure  
665 9. In the Ocitan Domain, VOL-OD samples share values with those of the San  
666 Sebastián orthogneiss, while OG-OD shares values with those of OG from the Central  
667 Iberian Zone.

668 The Zr vs. Nb diagram (Leat et al., 1986; modified by Piercy, 2011) (Fig. 11)  
669 illustrates how magmas evolved toward richer values in Zr and Nb, which is consistent  
670 with what it is observed in the Syme diagram (Fig. 9). Figure 11A documents how most  
671 samples show a general positive trend where two groups are distinguished. These  
672 different groups correspond to the OSS and Portalegre granites, highlighted in the  
673 figure. The two groups indicate a tendency toward alkaline magmas. In the rest of the  
674 diagrams, the groups from the Central Iberian Zone are projected in blue. Some  
675 samples, such as the Pyrenean G1, some Occitan VOL-OD samples and some  
676 Sardinian OG-UOS samples share the same affinity, clearly distinguished from the  
677 general geochemical trend exhibited by the Central Iberian Zone.

678 After plotting the data in a Zr vs. Ga/Al diagram (Whalen et al., 1987) (Fig. 12), the  
679 samples depict an intermediate character between alkaline and I&S. In the Central  
680 Iberian Zone, samples from the San Sebastián orthogneisses and Portalegre granites  
681 show characters of A-type granites, while the remaining samples display affinities of  
682 I&S-type granites. For the Central Iberian Zone, a clear magmatic shift toward more  
683 extensional geotectonic environments is characterized. For the eastern Pyrenees, we  
684 find the same situation than for the Central Iberian Zone, with a magmatic evolution  
685 toward A-granite type characteristics, indicating more extensional geotectonic  
686 environments. In the Occitan Domain, the samples show a clear I&S character. In the  
687 Sardinian case, the same seems to happen as in the Central Iberian Zone: the Upper  
688 Ordovician orthogneisses suggest a more extensional character.

689 In summary, all the reported diagrams point to a magmatic evolution through time,  
690 grading from arc to extensional geotectonic environments (with increased Zr/Ti ratios)



and to granite type-A characters. This geotectonic framework is consistent with that illustrated in Figure 9. The geochemical characters of these rocks show a rhyodacite to dacite composition, peraluminous and calc-alkaline K-rich character, and an arc-volcanic affinity for most of samples, but without intermediate rocks associated with andesitic types. Hence a change in time is documented toward more alkaline magmas.

696

#### 697 **4.2 Interpretation of $\varepsilon$ Nd values**

698

699  $\varepsilon$ Nd values are useful to interpret the nature of magmatic sources. Most samples of the  
700 above-reported groups show no meaningful differences in isotopic  $\varepsilon$ Nd values, and  
701 Nd<sub>CHUR</sub> model ages (Fig. 13). Some exceptions are related to granites from the  
702 southern Central Iberian Zone, which display positive values (from +2.6 to -2.4) and  
703 T<sub>DM</sub> values from 0.90 to 3.46 Ga. This feature could be interpreted as a more primitive  
704 nature of their parental magmas, even though the samples with highest T<sub>DM</sub> values are  
705 those that have higher <sup>147</sup>Sm/<sup>144</sup>Nd ratios (> 0.16; Table 1). On the other hand, very  
706 high values of the <sup>147</sup>Sm/<sup>144</sup>Nd ratio (> 0.13) could indicate post-magmatic hydrothermal  
707 alteration of the orthogneissic protoliths, as pointed out by Martínez et al. (2011).  
708 These are the case for samples from the Central Iberian Zone, VI-3 sample  
709 (Leucogneisses subgroup) and PORT2 and PORT15 of the Granites subgroup; as well  
710 as in the eastern Pyrenees, 99338 sample (G1 subgroup) and 100786 sample (Casemí  
711 subgroup). In Sardinia, CS5, CS8 and CC5 samples of the Upper Ordovician  
712 Orthogneisses subgroup show the highest values in T<sub>DM</sub> (Table 2; Fig. 13).

713 The volcanic rocks of the Central Iberian Zone display some differences following a  
714 N-S transect, being  $\varepsilon$ <sub>Nd</sub> values more negative in the north ( $\varepsilon$ Nd: -4.0 to -5.0) than in  
715 the south ( $\varepsilon$ Nd: -1.6 to -5.5). The isotopic signature of the Urra volcaniclastic rocks is  
716 compatible with magmas derived from young crustal rocks, with intermediate to felsic  
717 igneous compositions (Solá et al., 2008). The volcanic rocks of the northern Central  
718 Iberian Zone could be derived from old crustal rocks (Montero et al., 2007). The



719 isotopic composition of the granitoids from the southern Central Iberian Zone has more  
720 primitive characters than those of the northern Central Iberian Zone, suggesting  
721 different sources for both sides (Talavera et al., 2013). OSS shows lower inheritance  
722 patterns, more primitive Sr–Nd isotopic composition than other rocks of the Ollo de  
723 Sapo suite, and an age some 15 m.y. younger than most meta-igneous rocks of the  
724 Sanabria region (Montero et al., 2009), likely reflecting a greater mantle involvement in  
725 its genesis (Díez-Montes et al., 2008).

726 According to Talavera et al. (2013), the Cambro–Ordovician rocks of the Galicia-  
727 Trás-os-Montes Zone schistose area and the magmatic rocks of the northern Central  
728 Iberian Zone are contemporary. Both metavolcanic and metagranitic rocks almost  
729 share the same isotopic compositions.

730 The Upper Ordovician orthogneisses from the Occitan Domain show very little  
731 variation in  $\varepsilon$ Nd values (−3.5 to −4.0), typical of magmas derived from young crustal  
732 rocks. The variation in TDM values is also small (1.4 to 1.8 Ga) indicating short crustal  
733 residence times.

734 In Sardinia,  $\varepsilon$ Nd values present a greater variation (−1.6 to −3.3), but they are also  
735 included in the typical continental crustal range. As noted above, abnormal TDM values  
736 (between 1.2 to 4.5 Ga) may be due to post-magmatic hydrothermal alteration  
737 processes.

738

## 739 **5. Geodynamic scenario**

740

741 In the Iberian Massif, the Ediacaran–Cambrian transition was marked by  
742 paraconformities and angular discordances indicating the passage from Cadomian  
743 volcanic arc to rifting conditions. The axis of the so-called Ossa-Morena Rift lies along  
744 the homonymous Zone (Quesada, 1991; Sánchez-García et al., 2003, 2008, 2010)  
745 close to the remains of the Cadomian suture (Murphy et al., 2006). Rifting conditions  
746 were accompanied by a voluminous magmatism that changed from peraluminous acid



747 to bimodal (Sánchez-García et al., 2003, 2008, 2016, 2019). Some authors (Álvaro et  
748 al., 2014; Sánchez-García et al., 2019) propose that this rift resulted from a SW-to-NE  
749 inward migration, toward innermost parts of Gondwana, of rifting axes from the Anti-  
750 Atlas in Morocco to the Ossa-Morena Zone in the Iberian Massif. According to this  
751 proposal the rifting developed later (in Cambro-Ordovician times) in the Iberian,  
752 Armorican and Bohemian massifs.

753 The Furongian-Ordovician transition to drifting conditions is associated, in the  
754 Iberian Massif, Occitan Domain, Pyrenees and Sardinia, with a stepwise magmatic  
755 activity contemporaneous with the record of the Toledanian and Sardic unconformities.  
756 These, related to neither metamorphism nor penetrative deformations, are linked to  
757 uplift, erosion and irregularly distributed mesoscale deformation that gave rise to  
758 angular unconformities up to 90°. The time span involved in these gaps is similar (22  
759 m.y. in the Iberian Massif, 16–23 m.y. in the Pyrenees and 18 m.y. in Sardinia). This  
760 contrasts with the greater time span displayed by the magmatic activity (30–45 m.y.),  
761 which started before the unconformity formation (early Furongian in the Central Iberian  
762 Zone vs. Floian in the Pyrenees, Occitan Domain and Sardinia), pursuit during the  
763 unconformity formation (Furongian and early Tremadocian in the Central Iberian Zone  
764 vs. Floian-Darriwilian in the Pyrenees, Occitan Domain and Sardinia), and ended  
765 during the sealing of the uplifted and eroded palaeorelief (Tremadocian-Floian  
766 volcaniclastic rocks at the base of the Armorican Quartzite in the Central Iberian Zone  
767 vs. Sandbian-Katian volcanic rocks at the lowermost part of the Upper Ordovician  
768 successions in the Pyrenees, Occitan Domain and Sardinia; Gutiérrez-Alonso et al.,  
769 2007, 2016; Navidad et al., 2010; Martínez et al., 2011; Álvaro et al., 2016; Martí et al.,  
770 2019). In the Pyrenees, Upper Ordovician magmatism and sedimentation coexist with  
771 normal faults controlling marked thickness changes of the basal Upper Ordovician  
772 succession and cutting the lower part of this succession, the Sardic unconformity and  
773 the underlying Cambro-Ordovician sequence (Puddu et al., 2018, 2019).



775    *Toledanian Phase*

776

777    The Early Ordovician (Toledanian) magmatism of the Central Iberian Zone evolved to a  
778    typical passive-margin setting, with geochemical features dominated by acidic rocks,  
779    peraluminous and rich in K, and lacking any association with basic or intermediate  
780    rocks. Some of the orthogneisses of the Galicia-Trás-os-Montes Zone basal and  
781    allochthonous complex units share these same patterns. This fact has been interpreted  
782    by some authors as a basin environment subject to important episodes of crustal  
783    extension (Martínez-Catalán et al., 2007; Díez-Montes et al., 2010). In contrast,  
784    Villaseca et al. (2016) interpreted this absence as evidence against rifting conditions,  
785    though the absence of contemporary basic magmatism may be explained by the partial  
786    fusion of a thickened crust, through recycling of Neoproterozoic crustal materials. The  
787    thrust of a large metasedimentary sequence could generate dehydration and  
788    metasomatism of the rocks above this sequence, triggering partial fusion at different  
789    levels, although the increase in peraluminosity with the basicity of the ortogneisses is  
790    against any AFC process involving mantle materials. However, this increase in  
791    peraluminosity with the basicity has not been revealed in the samples studied above.  
792    Following Villaseca et al.'s (2016) model, a flat subduction of the southern part of the  
793    Central Iberian Zone would have taken place under its northern prolongation, whereas  
794    the reflection of such a subduction is not evident in the field. The calc-alkaline signature  
795    of this magmatism has also been taken into account as proof of its relationship with  
796    volcanic-arc environments (Valverde-Vaquero and Dunning, 2000). However, calc-  
797    alkaline features may be also interpreted as a result of a variable degree of continental  
798    crustal contamination and/or previously enriched mantle source (Sánchez-García et al.,  
799    2003, 2008, 2016, 2019; Díez-Montes et al., 2010). Finally, other granites not  
800    considered here of Tremadocian age have been reported in the southern Central  
801    Iberian Zone, such as the Oleo massif and the Beira Baixa-Central Extremadura,  
802    which display a I-type affinity (Antunes et al., 2009; Rubio Ordóñez et al., 2012). These



803 granites could represent different sources for the Ordovician magmatism in the Central  
804 Iberian Zone.

805 Sánchez-García et al. (2019) have proposed that the anomaly that produced the  
806 large magmatism throughout the Iberian Massif could have migrated from the rifting  
807 axis to inwards zones and the acid, peraluminous, K-rich rocks of Mid Ordovician in  
808 age should represent the initial stages of a new rifting pulse, resembling the  
809 peraluminous rocks of the Early Rift Event *sensu* Sánchez-García et al. (2003) from the  
810 Cambrian Epoch 2 of the Ossa-Morena Rift.

811 In the parautochthon of the Galicia-Trás-os-Montes Zone, the appearance of  
812 tholeiitic and alkaline-peralkaline magmatism in the Mid Ordovician would signal the  
813 first steps toward extensional conditions (Díez Fernández et al., 2012; Dias da Silva et  
814 al., 2016). In the Montagne Noire and the Mouthoumet massifs contemporaneous  
815 tholeiitic lavas indicate a similar change in the tectonic regimen (Álvaro et al., 2016).  
816 This gradual change in geodynamic conditions is also marked by the appearance of  
817 rocks with extensional characteristics in some of subgroups considered here, such as  
818 the Central Iberian Zone (San Sebastián orthogneisses), eastern Pyrenees (Casemí  
819 orthogneisses, and G1), volcanic rocks of the Occitan Domain, and the ortogneises and  
820 volcanic rocks from Sardinia.

821

822 *Sardic Phase*

823

824 In the eastern Pyrenees, two peaks of magmatic activity have been currently  
825 distinguished (Casas et al., 2019). Large Lower–Middle Ordovician peraluminous  
826 granite bodies are known representing the protoliths of numerous gneissic bodies with  
827 laccolithic morphologies. In the Canigó massif, the Upper Ordovician granite bodies  
828 (protholits of Cadí, Casemí, G1) are encased in sediments of the Canaveilles and  
829 Jujols groups. During this time span, there was generalized uplift and erosion that  
830 culminated with the onset of the Sardic unconformity. The Sardic Phase was



831 succeeded by an extensional pulsation related to the formation of normal faults  
832 affecting the pre-unconformity strata (Puddu et al., 2018, 2019). The volcanic arc  
833 signature can be explain by crustal recycling (Navidad et al., 2010; Casas et al., 2010;  
834 Martínez et al., 2011), as in the case of the Toledanian Phase in the Central Iberian  
835 Zone, although, according to Casas et al. (2019), the Pyrenees and the Catalan  
836 Coastal Ranges were probably fringing the Gondwana margin in a different position  
837 than that occupied by the Iberian Massif. As a whole, the Ordovician magmatism in the  
838 eastern Pyrenees lasted about 30 m.y., from ca 477 to 446 Ma, in a time span  
839 contemporaneous with the formation of the Sardic unconformity (Fig. 2). Recently,  
840 Puddu et al. (2019) proposed that a thermal doming, bracketted between 475 and 450  
841 Ma, should have stretched the Ordovician lithosphere. The emersion and denudation of  
842 the inherited Cambrian–Ordovician palaeorelief would have given rise to the onset of  
843 the Sardic unconformity. According to these authors, thermal doming triggered by hot  
844 mafic magma underplating may also be responsible for the late Early–Late Ordovician  
845 coeval magmatic activity.

846 In the Occitan Domain, there was a dramatic volcanic event in early Tremadocian  
847 times, with the uprising of basin floors and the subsequent effusion of abundant  
848 rhyolitic activities under subaerial explosive conditions (Larroque volcanosedimentary  
849 Complex in the Montagne Noire, and Davejean acidic volcanic counterpart in the  
850 Mouthoumet Massif). Pouclet el al., (2017) interpreted this as a delayed Ollo de Sapo-  
851 style outpouring where a massive crustal melting required a rather significant heat  
852 supply. Asthenospheric upwelling leading to the interplay of lithospheric doming,  
853 continental break-up, and a decompressionally driven mantle melting can explain such  
854 a great thermal anomaly. The magmatic products accumulated on the mantle-crust  
855 contact would provide enough heat transfer for crustal melting (Huppert and Sparks,  
856 1988). Subsequently, a post–Sardic reactivation of rifting conditions is documented in  
857 the Cabrières klippe (southern Montagne Noire) and the Mouthoumet massif. There, a  
858 Late Ordovician fault-controlled subsidence linked to the record of rift-related tholeiites



859 (Roque de Bandies and Villerouge formations) were contemporaneous with the record  
860 of the Hirnantian glaciation (Álvaro et al., 2016). Re-opening of rifting branches  
861 (Montagne Noire and Mouthoumet massifs) was geometrically recorded as onlapping  
862 patterns and final sealing of Sardic palaeoreliefes by Silurian and Lower Devonian  
863 strata.

864 Sardinia illustrates an almost complete record of the Variscan Belt (Carmignani et  
865 al., 1994; Rossi et al., 2009). Some plutonic orthogneises of the Inner Zone belong to  
866 this cycle, such as the orthogneises of Golfo Aranci (Giacomini et al., 2006). Gaggero  
867 et al. (2012) described three magmatic cycles. The first cycle is well represented in the  
868 Sarrabus unit by Furongian–Tremadocian volcanic and subvolcanic interbeds within a  
869 terrigenous succession (San Vito Formation) which is topped by the Sardic  
870 unconformity. Some plutonic orthogneises of the Inner Zone belong to this cycle, such  
871 as the orthogneises of Golfo Aranci (Giacomini et al., 2006) and the PB orthogneiss of  
872 Punta Bianca). The second Mid–Ordovician cycle, about 50 m.y. postdating the  
873 previous cycle, is of an arc-volcanic type with calc-alkaline affinity and acidic-to-  
874 intermediate composition. The acidic metavolcanites are referred in the literature as  
875 “porphyroids”, which crop out in the External Nappe Zone and some localities of the  
876 Inner Zone. The intermediate to basic derivates are widespread in Central Sardinia  
877 (Serra Tonnai Formation). Some plutonic rocks (Mt. Filau orthogneisses and Capo  
878 Spartivento) of the second cycle are discussed above. The third cycle consists of  
879 alkalic meta-epiclastites interbedded in post–Sandbian strata and metabasites marking  
880 the Ordovician/Silurian contact and reflecting rifting conditions. In this work only the first  
881 two cycles has been considered. Giacomini et al. (2006) cite coeval mafic rocks of  
882 felsic magmatism of Mid Ordovician age (Cortesogno et al., 2004; Palmeri et al., 2004;  
883 Giacomini et al., 2005), although they interpret a subduction scenario of the Hun terrain  
884 below Corsica and Sardinia in the Mid Ordovician.

885

886 *Intracrustal siliceous melts*



887

888 In this scenario, the key to generate large volumes of acidic rocks in an intraplate  
889 context would be the existence of a lower-middle crust, highly hydrated, in addition to a  
890 high heat flow, possibly caused by mafic magmas (Bryan et al., 2002; Díez-Montes,  
891 2007). This could be the scenario raised by the arrival of a thermal anomaly in a  
892 subduction-free area (Sánchez-García et al., 2003, 2008, 2019; Álvaro et al., 2016).  
893 The formation of large volumes of intracrustal siliceous melts could act as a viscous  
894 barrier, preventing the rise of mafic magmas within volcanic environments, and causing  
895 the underplating of these magmas at the contact between the lower crust and the  
896 mantle (Huppert and Sparks, 1988; Pankhurst et al., 1998; Bindeman and Valley,  
897 2003). The cooling of these magmas could lead to crustal thickening and in this case,  
898 the volcanic arc signature can be explained by crustal recycling (Navidad et al., 2010;  
899 Díez-Montes et al., 2010; Martínez et al., 2011).

900 Sánchez-García et al. (2019) have proposed that the anomaly that produced the  
901 large magmatism throughout the Iberian Massif could have migrated from the rifting  
902 axis to inwards zones and the acid, peraluminous, K-rich rocks of Mid Ordovician in  
903 age should represent the initial stages of a new rifting pulse, resembling the  
904 peraluminous rocks of the Early Rift Event *sensu* Sánchez-García et al. (2003) from the  
905 Cambrian Epoch 2 of the Ossa-Morena Rift. In the parautochthon of the Galicia-Trás-  
906 os-Montes Zone, the appearance of tholeiitic and alkaline-peralkaline magmatism in  
907 the Mid Ordovician would signal the first steps toward extensional conditions (Díez  
908 Fernández et al., 2012; Dias da Silva et al., 2016). In the Montagne Noire and the  
909 Mouthoumet massifs contemporaneous tholeiitic lavas indicate a similar change in the  
910 tectonic regimen (Álvaro et al., 2016). This change in geodynamic conditions is also  
911 marked by the appearance of rocks with extensional characteristics in some of  
912 subgroups considered here, such as the Central Iberian Zone (San Sebastián  
913 orthogneisses), eastern Pyrenees (Casemí orthogneisses, and G1), volcanic rocks of  
914 the Occitan Domain, and the ortogneisses and volcanic rocks from Sardinia. In the



915 Pyrenees, Puddu et al. (2019) proposed that a thermal doming, between 475 and 450  
916 Ma, should have stretched the Ordovician lithosphere leading to emersion and  
917 denudation of a Cambrian–Ordovician palaeorelief, and giving rise to the onset of the  
918 Sardic unconformity. According to these authors, thermal doming triggered by hot mafic  
919 magma underplating may also be responsible for the late Early–Late Ordovician coeval  
920 magmatic activity

921 A major continental break-up, leading to the so-called Tremadocian Tectonic Belt,  
922 was suggested by Pouclet et al. (2017), which initiated by upwelling of the  
923 asthenosphere and tectonic thinning of the lithosphere. Mantle-derived mafic magmas  
924 were underplated at the mantle-crust transition zone and intruded the crust. These  
925 magmas provided heat for crustal melting, which supplied the rhyolitic volcanism. After  
926 emptying the rhyolitic crustal reservoirs, the underlying mafic magmas finally rised and  
927 reached the surface. According to Pouclet et al. (2017), the acidic magmatic output  
928 associated with the onset of the Larroque metarhyolites resulted in massive crustal  
929 melting requiring a rather important heat supply. Asthenospheric upwelling leading to  
930 lithospheric doming, continental break-up, and a decompressional driven mantle  
931 melting can explain such a great thermal anomaly. Magmatic products accumulated on  
932 the mantle-crust contact providing enough heat transfer for crustal melting.

933

## 934 **6. Conclusions**

935

936 A geochemical comparison of 231 plutonic and volcanic samples of two major suites,  
937 Furongian–Mid Ordovician and Late Ordovician in age, and recorded in the Central  
938 Iberian and Galicia-Trás-os-Montes Zones of the Iberian Massif and in the eastern  
939 Pyrenees, Occitan Domain (Albigeois, Montagne Noire and Mouthoumet massifs) and  
940 Sardinia, is made in this work. The comparison points to a predominance of materials  
941 derived from the melting of metasedimentary rocks, peraluminous and rich in SiO<sub>2</sub> and  
942 K<sub>2</sub>O. The total content in REE is moderate to high. Most felsic rocks display similar



943 chondritic normalized REE patterns, with an enrichment of LREE relative to HREE,  
944 which should indicate the involvement of crustal materials in their parental magmas.  
945 Zr/TiO<sub>2</sub>, Zr/Nb, Nb/Y and Zr vs. Ga/Al ratios, and REE and  $\epsilon_{\text{Nd}}$  values reflect  
946 contemporaneous arc and extensional scenarios, which progressed to distinct  
947 extensional conditions finally associated with outpouring of mafic tholeiitic-dominant  
948 rifting lava flows. Magmatic events are contemporaneous with the formation of the  
949 Toledanian (Furongian-Early Ordovician) and Sardic (Early-Late Ordovician)  
950 unconformities, related to neither metamorphism nor penetrative deformation. The  
951 geochemical and structural framework precludes a subduction scenario reaching the  
952 crust in a magmatic arc to back-arc setting. On the contrary, it favours partial melting of  
953 sediments and/or granitoids in a continental lower crust triggered by the underplating of  
954 hot mafic magmas during extensional events related to the opening of the Rheic Ocean  
955 as a result of asthenospheric upwelling.

956

## 957 **7. Acknowledgements**

958

959 This paper is a contribution to projects CGL2017-87631-P and PGC2018-093903-B-  
960 C22 from Spanish Ministry of Science and Innovation.

961

962 **Data availability** - All data included in the paper and the Repository Data.

963

964 **Author contributions** - JJA, TSG and JMC: Methodology (Lead), Supervision (Lead),  
965 Writing – Original Draft (Lead), Writing – Review & Editing (Lead); CP, ADM, ML & GO:  
966 Methodology (Supporting), Supervision (Supporting), Writing – Original Draft  
967 (Supporting), Writing – Review & Editing (Supporting).

968

969 **Competing interests** - No competing interests

970



971    **References**

972

973    Alabouvette, B., Demange, M., Guérangé-Lozes, J., Ambert, P., 2003. Notice  
974    explicative de la carte géologique de Montpellier au 1/250 000. BRGM, Orléans.

975    Álvaro, J.J., Vizcaíno, D., 2018. The Furongian break-up (rift-drift) transition in the Anti-  
976    Atlas, Morocco. *J. Iberian Geol.* 44, 567–587.

977    Álvaro, J.J., Ferretti, F., González-Gómez, C., Serpagli, E., Tortello, M. F., Vecoli, M.,  
978    Vizcaíno, D., 2007. A review of the Late Cambrian (Furongian) palaeogeography in  
979    the western Mediterranean region, NW Gondwana. *Earth-Sci. Rev.* 85, 47–81.

980    Álvaro, J.J., Ezzouhairi, H., Ribeiro, M.L., Ramos, J.F., Solá, A.R., 2008. Early  
981    Ordovician volcanism of the Iberian Chains (NE Spain) and its influence on  
982    preservation of shell concentrations. *Bull. Soc. géol. France* 179(6), 569–581.

983    Álvaro, J.J., Bellido, F., Gasquet, D., Pereira, F., Quesada, C., Sánchez-García, T.,  
984    2014a. Diachronism of late Neoproterozoic–Cambrian arc-rift transition of North  
985    Gondwana: a comparison of Morocco and the Iberian Ossa-Morena Zone. *J. Afr.*  
986    *Earth Sci.* 98, 113–132.

987    Álvaro, J.J., Bauluz, B., Clausen, S., Devaere, L., Gil Imaz, A., Monceret, E., Vizcaíno,  
988    D., 2014b. Stratigraphy of the Cambrian–Lower Ordovician volcanosedimentary  
989    complexes, northern Montagne Noire, France. *Stratigraphy* 11, 83–96.

990    Álvaro, J.J., Colmenar, J., Monceret, E., Pouclet, A., Vizcaíno, D., 2016. Late  
991    Ordovician (post-Sardic) rifting branches in the North Gondwanan Montagne Noire  
992    and Mouthoumet massifs of southern France. *Tectonophysics* 681, 111–123.

993    Álvaro, J.J., Casas, J.M., Clausen, S., Quesada, C., 2018. Early Palaeozoic  
994    geodynamics in NW Gondwana. *J. Iberian Geol.* 44, 551–565.

995    Álvaro, J.J., Cortijo, I., Jensen, S., Lorenzo, S., Palacios, T., Pieren, A., 2019. Updated  
996    stratigraphic framework and biota of the Ediacaran and Terreneuvian in the Alcudia-  
997    Toledo Mountains of the Central Iberian Zone, Spain. *Est. Geol.* 75(2), e093.



- 998 Antunes, I.M.H.R., Neiva, A.M.R., Silva, M.M.V.G., Corfu, F., 2009. The genesis of I-  
999 and S-type granitoid rocks of the Early Ordovician Oledo pluton, Central Iberian  
1000 Zone (central Portugal). *Lithos* 111, 168–185.
- 1001 Arthaud, F., 1970. Etude tectonique et microtectonique comparée de deux domaines  
1002 hercyniens: les nappes de la Montagne Noire (France) et l'anticlinorium de  
1003 l'Iglesiente (Sardaigne). PhD, Univ. Montpellier.
- 1004 Ayora, C., 1980. Les concentrations métalliques de la Vall de Ribes. PhD, Univ.  
1005 Barcelona.
- 1006 Ballèvre, M., Fourcade S., Capdevila, R., Peucat, J.J., Cocherie, A., Mark Fanning, C.,  
1007 2012. Geochronology and geochemistry of Ordovician felsic volcanism in the  
1008 Southern Armorican Massif (Variscan belt, France): Implications for the breakup of  
1009 Gondwana. *Gondwana Res.* 21, 1019–1036.
- 1010 Barca, S., 1991. Phénomènes de resédimentation et flysch hercynien à faciès Culm  
1011 dans le “synclinal du Sarrabus” (SE de la Sardaigne, Italie). *C. R. Acad. Sci., Paris*  
1012 313(2), 1051–1057.
- 1013 Barca, S., Cherchi, A., 2004. Regional geological setting. In: Barca, S., Cherchi, A.  
1014 (eds.), *Sardinian Palaeozoic Basement and its Meso-Cainozoic Cover (Italy)*. 32nd  
1015 Int. Geol. Congress. Field Trip Guide Book–P39 (5), 3–8.
- 1016 Barca, S., Carmignani, L., Maxia, M., Oggiano, G., Pertusati, P.C., 1986. The Geology  
1017 of Sarrabus. In: *Guide-Book to the Excursion on the Paleozoic Basement of Sardinia*  
1018 (Carmignani, L., Cocozza, T., Ghezzo, C., Pertusati, P.C., Ricci, C.A., eds.). IGCP  
1019 *Newsl.*, Spec. Iss. 5, 51–60.
- 1020 Barca, S., Cocozza, T., Del Rio, M., Pillola, G.L., Pittau Demelia, P., 1987. Datation de  
1021 l'Ordovicien inférieur par *Dictyonema flabelliforme* et acritarches dans la partie  
1022 supérieure de la formation “cambrienne” de Cabitza (SW de la Sardaigne, Italie):  
1023 conséquences géodynamiques. *C. R. Acad. Sci., Paris* 305(2), 1109–1113.
- 1024 Barca, S., Del Rio, M., Pittau Demelia, P., 1988. New geological and stratigraphical  
1025 data and discovery of Lower Ordovician acritarchs in the San Vito Sandstone of the



- 1026 Genn'Argiolas Unit (Sarrabus, Southeastern Sardinia). Riv. It. Paleontol. Stratigr. 94,  
1027 339–360.
- 1028 Bea, F., Montero, P., Talavera, C., Zinger, T., 2006. A revised Ordovician age for the  
1029 Miranda do Douro orthogneiss, Portugal. Zircon U–Pb ion-microprobe and LA–  
1030 ICPMS dating. Geol. Acta 4, 395–401.
- 1031 Bea, F., Montero, P., González Lodeiro, F., Talavera, C., 2007. Zircon inheritance  
1032 reveals exceptionally fast crustal magma generation processes in Central Iberia  
1033 during the Cambro–Ordovician. J. Petrol. 48, 2327–2339
- 1034 Bé Mézème, E., 2005. Contribution de la géochronologie U–Th–Pb sur monazite à la  
1035 compréhension de la fusion crustale dans la chaîne Hercynienne française et  
1036 implication géodynamique. PhD, Univ. Orléans.
- 1037 Bindeman, I.N., Valley, J.W., 2003. Rapid generation of both high- and low- $\delta^{18}\text{O}$ , large-  
1038 volume silicic magmas at the Timber Mountain/Oasis Valley caldera complex,  
1039 Nevada. Geol. Soc. Am. Bull. 115(5), 581–595.
- 1040 Boni, M., 1986. The Permo–Triassic vein and paleokarst ores in southwest Sardinia:  
1041 contribution of fluid inclusion studies to their genesis and paleoenvironment. Mineral.  
1042 Deposita 21, 53–62.
- 1043 Boni, M., Koeppel, V., 1985. Ore-lead isotope pattern from the Iglesiente-Sulcis area  
1044 (SW Sardinia) and the problem of remobilization of metals. Mineral. Deposita 20,  
1045 185–193.
- 1046 Bryan, S.E., Riley, T.R., Jerram, D.A., Stephens, Ch.J., Leat, Ph.T., 2002. Silicic  
1047 volcanism: An undervalued component of large igneous provinces and volcanic  
1048 rifted margins. In: Volcanic Rifted Margins (Menzies, M.A., Klemperer, S.L., Ebinger,  
1049 C.J., Baker, J., eds.). Geol. Soc. Am., Spec. Pap. 362, 99–120.
- 1050 Calvet, P., Lapierre, H., Chavet, J., 1988. Diversité du volcanisme Ordovicien dans la  
1051 région de Pierrefitte (Hautes Pyrénées): rhyolites calco-alcalines et basaltes  
1052 alcalins. C. R. Acad. Sci., Paris 307, 805–812.



- 1053 Calvino, F., 1972. Note Illustrative della Carta Geologica d'Italia, Foglio 227 –  
1054 Muravera. Servizio Geologico d'Italia, Roma, 60 p.
- 1055 Carmignani, L., Cocozza, T., Ghezzo, C., Pertusati, P.C., Ricci, C.A., 1986. Guide-  
1056 book to the Excursion on the Palaeozoic Basement of Sardinia. IGCP Project no. 5,  
1057 Newsl. Spec. Iss., 1–102.
- 1058 Carmignani, L., Pertusati, P.C., Barca, S., Carosi, R., Di Pisa, A., Gattiglio, M., et al.,  
1059 1992. Struttura della Catena Ercinica in Sardegna. Guida all'escursione del Gruppo  
1060 Informali di Geologia Strutturale in Sardegna, 24–29 (Maggio), 1–177.
- 1061 Carmignani, L., Carosi, R., Di Pisa, A., Gattiglio, M., Musumeci, G., Oggiano, G. et al.,  
1062 1994. The Hercynian chain in Sardinia (Italy). *Geodin. Acta* 7, 31–47.
- 1063 Carmignani, L., Oggiano, G., Barca, S., Conti, P., Salvadori, I., Eltrudis, A. et al. 2001.  
1064 Geologia della Sardegna. Note illustrative della Carta Geologica della Sardegna a  
1065 scala 1:200.000. Memorie Descrittive della Carta Geologica d'Italia, Servizio  
1066 Geologico 60, 1–283. Instituto Poligrafico e Zecca dello Stato, Roma.
- 1067 Caron, C., Lancelot, J., Omenetto, P., Orgeval, J.J., 1997. Role of the Sardic tectonic  
1068 phase in the metallogenesis of SW Sardinia (Iglesiente): lead isotope evidence.  
1069 European J. Miner. 9, 1005–1016.
- 1070 Casas, J.M., 2010. Ordovician deformations in the Pyrenees: new insights into the  
1071 significance of pre-Variscan ('sardic') tectonics. *Geol. Mag.* 147, 674–689.
- 1072 Casas, J.M., Fernández, O., 2007. On the Upper Ordovician unconformity in the  
1073 Pyrenees: New evidence from the La Cerdanya area. *Geol. Acta* 5, 193–198.
- 1074 Casas, J.M., Murphy, J.B. 2018. Unfolding the arc: the use of pre-orogenic constraints  
1075 to assess the evolution of the Variscan belt in Western Europe. *Tectonophysics* 736,  
1076 47–61.
- 1077 Casas, J.M., Palacios, T., 2012. First biostratigraphical constraints on the pre–Upper  
1078 Ordovician sequences of the Pyrenees based on organic-walled microfossils. *C. R.  
1079 Geosci.* 344, 50–56.



- 1080 Casas, J.M., Castiñeiras, P., Navidad, M., Liesa, M., Carreras, J., 2010. New insights  
1081 into the Late Ordovician magmatism in the Eastern Pyrenees: U–Pb SHRIMP zircon  
1082 data from the Canigó massif. *Gondwana Res.* 17, 317–324.
- 1083 Casas, J.M., Álvaro, J.J., Clausen, S., Padel, M., Puddu, C., Sanz-López, J., Sánchez-  
1084 García, T., Navidad, M., Castiñeiras, P., Liesa, M., 2019. Palaeozoic basement of  
1085 the Pyrenees. In: *The Geology of Iberia: A Geodynamic Approach* (Quesada, C.,  
1086 Oliveira, J.T., eds.). *Regional Geology Reviews*, vol. 2, 229–259. Springer,  
1087 Heidelberg.
- 1088 Castiñeiras, P., Villaseca, C., Barbero, L., Martín-Romera, C., 2008a. SHRIMP U–Pb  
1089 zircon dating of anatexis in high-grade migmatite complexes of Central Spain:  
1090 implications in the Hercynian evolution of Central Iberia. *Int. J. Earth Sci.* 97, 35–50.
- 1091 Castiñeiras, P., Navidad, M., Liesa, M., Carreras, J., Casas, J.M., 2008b. U–Pb zircon  
1092 ages (SHRIMP) for Cadomian and Lower Ordovician magmatism in the Eastern  
1093 Pyrenees: new insights in the pre–Variscan evolution of the northern Gondwana  
1094 margin. *Tectonophysics* 46, 228–239.
- 1095 Castro, A., García-Casco, A., Fernández, C., Corretgé, L.G., Moreno-Ventas, I., Gerya,  
1096 T., Löw, I., 2009. Ordovician ferrosilicic magmas: experimental evidence for  
1097 ultrahigh temperatures affecting a metagreywacke source. *Gondwana Res.* 16, 622–  
1098 632
- 1099 Charles, N., Faure, M., Chen, Y., 2008. The emplacement of the Montagne Noire axial  
1100 zone (French Massif Central): New insights from petro-textural, geochronological  
1101 and AMS studies. *22ème Réunion des Sciences de la Terre*, Nancy, 155.
- 1102 Charles, N., Faure, M., Chen, Y., 2009. The Montagne Noire migmatitic dome  
1103 emplacement (French Massif Central): New insights from petrofabric and AMS  
1104 studies. *J. Struct. Geol.* 31, 1423–1440.
- 1105 Clariana, P., Valverde-Vaquero, P., Rubio-Ordóñez, A., Beranoaguirre, A., García-  
1106 Sansegundo, J., 2018. Pre–Variscan tectonic events and Late Ordovician



- 1107 magmatism in the Central Pyrenees: U–Pb age and Hf in zircon isotopic signature  
1108 from subvolcanic sills in the Pallaresa massif. *J. Iberian Geol.* 44, 589–601.
- 1109 Cocco, F., Funedda, A., 2011. New data on the pre–Middle Ordovician deformation in  
1110 SE Sardinia: a preliminary note. *Rend. online Soc. Geol. It.* 15, 34–36.
- 1111 Cocco, F., Funedda, A., 2017. The Sardic Phase: field evidence of Ordovician tectonics  
1112 in SE Sardinia. *Italy. Geol. Mag.* 156, 25–38.
- 1113 Cocco, F., Oggiano, G., Funedda, A., Loi, A., Casini, L., 2018. Stratigraphic, magmatic  
1114 and structural features of Ordovician tectonics in Sardinia (Italy): a review. *J. Iberian  
1115 Geol.* 44, 619–639.
- 1116 Cocherie, A., 2003. Datation avec le SHRIMP II du métagranite oeillé du Somain-  
1117 Montagne Noire. *C. R. technique ANA–ISO/NT, BRGM.*
- 1118 Cocherie, A., Baudin, T., Guerrot, C., Autran, A., Fanning, M.C., Laumonier, B., 2005.  
1119 U–Pb zircon (ID–TIMS and SHRIMP) evidence for the early Ordovician intrusion of  
1120 metagranites in the late Proterozoic Canaveilles Group of the Pyrenees and the  
1121 Montagne Noire (France). *Bull. Soc. géol. France* 176, 269–282.
- 1122 Cortesogno, L., Gaggero, L., Oggiano, G., Paquette, J.L., 2004. Different tectono-  
1123 thermal evolution paths in eclogitic rocks from the Axial Zone of the Variscan Chain  
1124 in Sardinia (Italy) compared with the Ligurian Alps. *Ophioliti* 29, 125–144.
- 1125 Cruciani, G., Franceschelli, M., Musumeci, G., Spano, M.E., Tiepolo, M., 2013. U–Pb  
1126 zircon dating and nature of metavolcanics and metarkoses from the Monte Grighini  
1127 Unit: new insights on Late Ordovician magmatism in the Variscan belt in Sardinia,  
1128 Italy. *Int. J. Earth Sci.* 102, 2077–2096.
- 1129 Cruciani, G., Franceschelli, M., Puxeddu, M., Tiepolo, M., 2018. Metavolcanics from  
1130 Capo Malfatano, SW Sardinia, Italy: New insight on the age and nature of  
1131 Ordovician volcanism in the Variscan foreland zone. *Geol. J.* 53(4), 1573–1585.
- 1132 Demange, M., 1999. Evolution tectonique de la Montagne noire: un modèle en  
1133 transpression. *C. R. Acad. Sci., Paris* 329, 823–829.



- 1134 Demange, M., Guérangé-Lozes, J., Guérangé, B., 1996. Notice explicative de la feuille  
1135 de Lacaune (987) au 1:50 000. BRGM, Orléans.
- 1136 Denèle, Y., Barbey, P., Deloule, E., Pelleter, E., Olivier, Ph., Gleizes, G., 2009. Middle  
1137 Ordovician U–Pb age of the Aston and Hospitalet orthogneissic laccoliths: their role  
1138 in the Variscan evolution of the Pyrenees. Bull. Soc. géol. France 180, 209–221.
- 1139 DePaolo, D.J., 1981. Neodymium isotopes in the Colorado Front Range and crust-  
1140 mantle evolution in the Proterozoic. Nature 291, 193–196.
- 1141 DePaolo, D.J., 1988. Neodymium isotope geochemistry. An introduction. Minerals and  
1142 Rocks Series 20, 1–187. Springer-Verlag, Berlin.
- 1143
- 1144 DePaolo, D.J., Wasserburg, G.J., 1976. Nd isotopic variations and petrogenetic  
1145 models. Geophys. Res. Lett. 3(5), 249–252.
- 1146 Dias da Silva, I., Valverde-Vaquero, P., González-Clavijo, E., Díez-Montes, A.,  
1147 Martínez-Catalán, J.R., 2012. Structural and stratigraphical significance of U–Pb  
1148 ages from the Saldanha and Mora volcanic complexes (NE Portugal, Iberian  
1149 Variscides). Géol. France 1, 105–106.
- 1150 Dias da Silva I., Valverde-Vaquero, P., González Clavijo E., Díez-Montes A., Martínez  
1151 Catalán J.R., 2014. Structural and stratigraphical significance of U–Pb ages from the  
1152 Mora and Saldanha volcanic complexes (NE Portugal, Iberian Variscides). In:  
1153 Schulmann, K., Martínez Catalán, J. R., Lardeaux, J. M., Janousek, V., Oggiano, G.,  
1154 (eds.), The Variscan Orogeny: Extent, Timescale and the Formation of the  
1155 European Crust. Geol. Soc., London, Spec. Publ. 405,  
1156 <http://dx.doi.org/10.1144/SP405.3>
- 1157 Dias da Silva, I., Díez Fernández, R., Díez Montes, A., González Clavijo, E., Foster,  
1158 D.A., 2016. Magmatic evolution in the N-Gondwana margin related to the opening of  
1159 the Rheic Ocean – evidence from the Upper Parautochthon of the Galicia-Trás-os-  
1160 Montes Zone and from the Central Iberian Zone (NW Iberian Massif). Int. J. Earth  
1161 Sci. 105, 1127–1151.



- 1162 Díaz-Alvarado, J., Fernández, C., Chichorro, M., Castro, A., Pereira, M.F., 2016.  
1163 Tracing the Cambro–Ordovician ferrosilicic to calc-alkaline magmatic association in  
1164 Iberia by *in situ* U–Pb SHRIMP zircon geochronology (Gredos massif, Spanish  
1165 Central System batholith). *Tectonophysics* 681, 95–110.
- 1166 Díez Fernández, R., Castiñeiras, P., Gómez Barreiro, J., 2012. Age constraints on  
1167 Lower Paleozoic convection system: Magmatic events in the NW Iberian Gondwana  
1168 margin. *Gondwana Res.* 21, 1066–1079.
- 1169 Díez-Montes, A., 2007. La Geología del Dominio “Ollo de Sapo” en las Comarcas de  
1170 Sanabria y Terra do Bolo. PhD, Univ. Salamanca. Laboratorio Xelóxico de Laxe,  
1171 Serie Nova Terra no. 34, A Coruña.
- 1172 Díez Montes, A., Martínez Catalán, J.R., Bellido Mulas, F., 2010. Role of the Ollo de  
1173 Sapo massive felsic volcanism of NW Iberia in the Early Ordovician dynamics of  
1174 northern Gondwana. *Gondwana Res.* 17, 363–376.
- 1175 Di Pisa, A., Gattiglio, M., Oggiano, G., 1992. Pre–Hercynian magmatic activity in the  
1176 nappe zone (internal and external) of Sardinia: evidence of two within plate basaltic  
1177 cycles. In: Contributions to the Geology of Italy with Special Regard to the Paleozoic  
1178 Basements (Carmignani, L., Sassi, F.P., eds.). *Newslett. IGCP 276*, 107–116.
- 1179 Echtler, H., Malavieille, J., 1990. Extensional tectonics, basement uplift and Stephano–  
1180 Permian collapse basin in a late Variscan metamorphic core complex (Montagne  
1181 Noire, southern Massif Central). *Tectonophysics* 177, 125–138.
- 1182 El Korh, A., Schmidt , S.Th., Ballèvre, M., Ulianov, A., Bruguier, O., 2012. Discovery of  
1183 an albite gneiss from the Ile de Groix (Armorican Massif, France): geochemistry and  
1184 LA–ICP–MS U–Pb geochronology of its Ordovician protolith. *Int. J. Earth Sci.* 101,  
1185 1169–1190.
- 1186 Engel,W., Feist, R., Franke,W., 1980. Le Carbonifère anté–stéphanien de la Montagne  
1187 Noire: rapports entre mise en place des nappes et sédimentation. *Bull. BRGM* 2,  
1188 341–389.



- 1189 Farias, P., Ordoñez-Casado, B., Marcos, A., Rubio-Ordóñez, A., Fanning, C.M., 2014.  
1190 U-Pb zircon SHRIMP evidence for Cambrian volcanism in the Schistose Domain  
1191 within the Galicia-Trás-os-Montes Zone (Variscan Orogen, NW Iberian Peninsula).  
1192 Geol. Acta 12(3), 209–218.
- 1193 Faure, M., Ledru, P., Lardeaux, J.M., Matte, P., 2004. Paleozoic orogenies in the  
1194 French Massif Central. A cross section from Béziers to Lyon. 32nd Int. Geol.  
1195 Congress Florence (Italy), Field-trip guide book, 40 p.
- 1196 Feist, R., Galtier, J., 1985. Découverte de flores d'âge namurien probable dans le  
1197 flysch à olistolithes de Cabrières (Hérault). Implications sur la durée de la  
1198 sédimentation synorogénique dans la Montagne Noire (France Méridionale). C. R.  
1199 Acad. Sci., Paris 300, 207–212.
- 1200 Franz, L., Romer, R.L., 2007. Caledonian high-pressure metamorphism in the Strona-  
1201 Ceneri-Zone (Southern Alps of southern Switzerland and northern Italy). Swiss J.  
1202 Geosci. 100, 457–467.
- 1203 Friedl, G., Finger, F., Paquette, J.L., von Quadt, A., McNaughton, N.J., Fletcher, I.R.,  
1204 2004. Pre-Variscan geological events in the Austrian part of the Bohemian Massif  
1205 deduced from U-Pb zircon ages. Int. J. Earth Sci. 93, 802–823
- 1206 Funedda, A., Oggiano, G., 2009. Outline of the Variscan basement of Sardinia. In: The  
1207 Silurian of Sardinia. Volume in Honour of Enrico Serpagli (Corradini, C., Ferretti, A.,  
1208 Štorch, P., eds.). Rend. Soc. Paleontol. It. 3, 23–35.
- 1209 Gaggero L., Oggiano G., Funedda A., Buzzi L., 2012. Rifting and arc-related Early  
1210 Paleozoic volcanism along the North Gondwana margin: Geochemical and  
1211 geological evidence from Sardinia (Italy). J. Geol. 120, 273–292.
- 1212 García-Arias, M., Díez-Montes, A., Villaseca, C., Blanco-Quintero, I.F. 2018. The  
1213 Cambro-Ordovician Ollo de Sapo magmatism in the Iberian Massif and its Variscan  
1214 evolution: A review. Earth-Sci. Rev. 176, 345–372.
- 1215 Gèze, B., 1949. Etude géologique de la Montagne Noire et des Cévennes  
1216 méridionales. Mém. Soc. géol. France 62, 1–215.



- 1217 Giacomini, F., Bomparola, R.M., Ghezzo, C., 2005. Petrology and geochronology of  
1218 metabasites with eclogite facies relics from NE Sardinia: constraints for the  
1219 Palaeozoic evolution of Southern Europe. *Lithos* 82, 221–248.
- 1220 Giacomini, F., Bomparola, R.M., Ghezzo, C., Guldbransen, H., 2006. The geodynamic  
1221 evolution of the Southern European Variscides: constraints from the U/Pb  
1222 geochronology and geochemistry of the lower Palaeozoic magmatic-sedimentary  
1223 sequences of Sardinia (Italy). *Contrib. Miner. Petr.* 152, 19–42.
- 1224 Guérangé-Lozes, J., Alabouvette, B., 1999. Notice explicative, Carte géol. France (1/50  
1225 000), feuille Saint-Sernin-sur-Rance (960). BRGM, Orléans, 84 p.
- 1226 Guérangé-Lozes, J., Guérangé, B., Mouline, M.P., Delsahut, B., 1996. Notice  
1227 explicative, Carte géol. France (1/50 000), feuille Réalmont (959). BRGM, Orléans,  
1228 78 p.
- 1229 Guitard, G., 1970. Le métamorphisme hercynien mésozonal et les gneiss oeillés du  
1230 masif du Canigou (Pyrénées orientales). *Mém. BRGM* 63, 1–353.
- 1231 Gutiérrez-Alonso, G., Fernández-Suárez, J., Gutiérrez-Marco, J.C., Corfu, F., Murphy,  
1232 J.B., Suárez Martínez, S., 2007. U–Pb depositional age for the upper Barrios  
1233 Formation (Armorican Quartzite facies) in the Cantabrian zone of Iberia: implications  
1234 for stratigraphic correlation and paleogeography. In: *The Evolution of the Rheic*  
1235 *Ocean: from Avalonian–Cadomian Active Margin to Alleghenian–Variscan Collision*  
1236 (Linnemann, R.D., Nance, P., Kraft, G.Z., eds.). *Geol. Soc. Am.*, London, 287–296.
- 1237 Gutiérrez-Alonso, G., Gutiérrez-Marco, J.C., Fernández-Suárez, J., Bernárdez, E.,  
1238 Corfu, F., 2016. Was there a super-eruption on the Gondwanan coast 477 Ma ago?  
1239 *Tectonophysics* 681, 85–94.
- 1240 Gutiérrez-Marco, J.C., Piçarra, J.M., Meireles, C.A., Cózar, P., García-Bellido, D.C.,  
1241 Pereira, Z. et al., 2019. Early Ordovician–Devonian Passive margin stage in the  
1242 Gondwanan units of the Iberian massif. In: *The Geology of Iberia: A Geodynamic*  
1243 *Approach* (Quesada, C., Oliveira, J.T., eds.). *Regional Geology Reviews*, vol. 2, 75–  
1244 98. Springer, Heidelberg.



- 1245 Hartevelt, J.J.A., 1970. Geology of the upper Segre and Valira valleys, central  
1246 Pyrenees, Andorra/Spain. *Leid. Geol. Meded.* 45, 167–236.
- 1247 Helbing, H., Tiepolo, M., 2005. Age determination of Ordovician magmatism in NE  
1248 Sardinia and its bearing on Variscan basement evolution. *J. Geol. Soc.* 162, 689–  
1249 700.
- 1250 Huppert, H.E., Sparks, R.S.J., 1988. The generation of granitic magmas by intrusion of  
1251 basalt into continental crust. *J. Petrol.* 29, 599–624.
- 1252 Jégouzo, P., Peucat, J.J., Audren, C., 1986. Caractérisation et signification  
1253 géodynamique des orthogneiss calco-alcalins d'âge ordovicien de Bretagne  
1254 méridionale. *Bull. Soc. géol. France* 2, 839–848.
- 1255 Kröner, A., Willner, A.P., 1998. Time of formation and peak of Variscan HP-HT  
1256 metamorphism of quartz-feldspar rocks in the central Erzgebirge, Saxony, Germany.  
1257 *Contrib. Mineral. Petrol.* 132, 1–20
- 1258 Lancelot, J., Allegret, A., Iglesias Ponce de León, M., 1985. Outline of Upper  
1259 Precambrian and Lower Paleozoic evolution of the Iberian Peninsula according to  
1260 U–Pb dating of zircons. *Earth Planet. Sci. Lett.* 74, 325–337.
- 1261 Laske, R., Bechstädt, T., Boni, M., 1994. The post-Sardic Ordovician series. In:  
1262 Sedimentological, stratigraphical and ore deposits field guide of the autochthonous  
1263 Cambro-Ordovician of Southeastern Sardinia (Bechstädt, T., Boni, M., eds.).  
1264 *Memorie descrittive della carta geologica d'Italia* 48, 115–146.
- 1265 Leat, P.T., Jackson, S.E., Thorpe, R.S., Stillman, C.J., 1986. Geochemistry of bimodal  
1266 basalt-subalkaline/peralkaline rhyolite provinces within the Southern British  
1267 Caledonides. *J. Geol. Soc.* 143, 259–273.
- 1268 Le Corre, C., Auvray, B., Ballèvre, M., Robardet, M., 1991. Le Massif Armorican. *Sci.*  
1269 *Géol.*, *Bull.* 44, 31–103.
- 1270 Lentz, D., 1996. U, Mo and REE mineralization in late-tectonic granite pegmatites,  
1271 south-west Grenville Province, Canada. *Ore Geol. Rev.* 11, 197–227.



- 1272 Leone, F., Hamman, W., Laske, R., Serpagli, E., Villas, E., 1991. Lithostratigraphic  
1273 units and biostratigraphy of the post-Sardic Ordovician sequence in south-west  
1274 Sardinia. *Boll. Soc. Paleontol. It.* 30, 201–235.
- 1275 Leone, F., Ferretti, A., Hammann, W., Loi, A., Pillola, G.L., Serpagli, E., 2002. A  
1276 general view of the post-Sardic Ordovician sequence from SW Sardinia. *Rend. Soc.*  
1277 *Paleontol. It.* 1, 51–68.
- 1278 Lescuyer, J.L., Cocherie, A., 1992. Datation sur monozircons des métadacites de  
1279 Séries: arguments pour un âge protérozoïque terminal des “schistes X” de la  
1280 Montagne Noire (Massif central français). *C. R. Acad. Sci., Paris (sér. 2)* 314, 1071–  
1281 1077.
- 1282 Liesa, M., Carreras, J., Castiñeiras, P., Casas, J.M., Navidad, M., Vilà, M., 2011. U–Pb  
1283 zircon age of Ordovician magmatism in the Albera Massif (Eastern Pyrenees). *Geol.*  
1284 *Acta* 9, 1–9.
- 1285 Linnemann, U., Gehmlich, M., Tichomirowa, M., Buschmann, B., Nasdala, L., Jonas, P.  
1286 et al. 2000. From Cadomian subduction to early Palaeozoic rifting: the evolution of  
1287 Saxo-Thuringia at the margin of Gondwana in the light of single zircon  
1288 geochronology and basin development (Central European Variscides, Germany). In:  
1289 Orogenic Processes: Quantification and Modelling in the Variscan Belt (Franke, W.,  
1290 Haak, V., Oncken, O., Tanner, D., eds.). *Geol. Soc., London, Spec. Publ.* 179, 131–  
1291 153.
- 1292 Loi, A., Dabard, M.P., 1997. Zircon typology and geochemistry in the palaeogeographic  
1293 reconstruction of the Late Ordovician of Sardinia (Italy). *Sediment. Geol.* 112, 263–  
1294 279.
- 1295 Loi, A., Barca, S., Chauvel, J.J., Dabard, M.P., Leone, F., 1992. Analyse de la  
1296 sédimentation post-phase sarde les dépôts initiaux à placers du SE de la Sardaigne.  
1297 *C. R. Soc. géol. France (sér. 2)* 315, 1357–1364.
- 1298 López-Sánchez, M.A., Iriondo, A., Marcos, A., Martínez, F.J., 2015. A U–Pb zircon age  
1299 (479 ± 5 Ma) from the uppermost layers of the Ollo de Sapo Formation near Viveiro



- 1300 (NW Spain): implications for the duration of rifting-related Cambro-Ordovician  
1301 volcanism in Iberia. *Geol. Mag.* 152, 341–350.
- 1302 Ludwig, K.R., Turi, B., 1989. Paleozoic age of the Capo Spartivento Orthogneiss,  
1303 Sardinia, Italy. *Chem. Geol.* 79, 147–153.
- 1304 Margalef, A., Castiñeiras, P., Casas, J.M., Navidad, M., Liesa, M., Linnemann, U.,  
1305 Hofmann, M., Gärtner, A., 2016. Detrital zircons from the Ordovician rocks of the  
1306 Pyrenees: Geochronological constraints and provenance. *Tectonophysics* 681, 124–  
1307 134.
- 1308 Marini, F., 1988. “Phase” sarde et distension ordovicienne du domaine sud-varisque,  
1309 effets de point chaud? Une hypothèse fondée sur les données nouvelles du  
1310 volcanisme albigeois. *C. R. Acad. Sci., Paris (sér. 2)* 306, 443–450.
- 1311 Martí, J., Muñoz, J.A., Vaquer, R., 1986. Les roches volcaniques de l’Ordovicien  
1312 supérieur de la région de Ribes de Freser-Rocabruna (Pyrénées catalanes):  
1313 caractères et signification. *C. R. Acad. Sci., Paris* 302, 1237–1242.
- 1314 Martí, J., Solari, L., Casas, J.M., Chichorro, M., 2019. New late Middle to early Late  
1315 Ordovician U–Pb zircon ages of extension-related felsic volcanic rocks in the  
1316 Eastern Pyrenees (NE Iberia): tectonic implications. *Geol. Mag.* 156(10), 1783–  
1317 1792.
- 1318 Martínez, F., Iriondo, A., Dietsch, C., Aleinikoff, J.N., Peucat, J.J., Cirès, J., Reche, J.,  
1319 Capdevila, R., 2011. U–Pb SHRIMP–RG zircon ages and Nd signature of lower  
1320 Paleozoic rifting-related magmatism in the Variscan basement of the Eastern  
1321 Pyrenees. *Lithos* 127, 10–23.
- 1322 Martínez Catalán, J.R., Arenas, R., Díaz García, F., Gómez Barreiro, J., González  
1323 Cuadra, P., Abati, J. et al. 2007. Space and time in the tectonic evolution of the  
1324 northwestern Iberian Massif. Implications for the comprehension of the Variscan  
1325 belt. In: 4–D Framework of Continental Crust (Hatcher, R.D.Jr., Carlson, M.P.,  
1326 McBride, J.H., Martínez Catalán, J.R., eds.). *Geol. Soc. Am., Mem.* 200, 403–423.



- 1327 Martini, I.P., Tongiorgi, M., Oggiano, G., Cocozza, T., 1991. Ordovician alluvial fan to  
1328 marine shelf transition in SW Sardinia, Western Mediterranean Sea: tectonically  
1329 (“Sardic” phase”) influenced clastic sedimentation. *Sediment. Geol.* 72, 97–115.
- 1330 McDougall, N., Brenchley, P.J., Rebelo, J.A., Romano, M., 1987. Fans and fan deltas –  
1331 precursors to the Armorican Quartzite (Ordovician) in western Iberia. *Geol. Mag.*  
1332 124, 347–359.
- 1333 Mezger, J., Gerdes, A., 2016. Early Variscan (Visean) granites in the core of central  
1334 Pyrenean gneiss domes: implications from laser ablation U–Pb and Th–Pb studies.  
1335 *Gondwana Res.* 29, 181–198.
- 1336 Mingram, B., Kröner, A., Hegner, E., Krentz, O., 2004. Zircon ages, geochemistry, and  
1337 Nd isotopic systematics of pre–Variscan orthogneisses from the Erzgebirge, Saxony  
1338 (Germany), and geodynamic interpretation. *Int. J. Earth Sci.* 93, 706–727.
- 1339 Montero, P., Bea, F., González-Lodeiro, F., Talavera, C., Whitehouse, M.J., 2007.  
1340 Zircon ages of the metavolcanic rocks and metagranites of the Ollo de Sapo Domain  
1341 in central Spain: implications for the Neoproterozoic to Early Palaeozoic evolution of  
1342 Iberia. *Geol. Mag.* 144, 963–976.
- 1343 Montero, P., Talavera, C., Bea, F., Lodeiro, F.G., Whitehouse, M.J., 2009. Zircon  
1344 geochronology of the Ollo de Sapo Formation and the age of the Cambro–  
1345 Ordovician rifting in Iberia. *J. Geol.* 117, 174–191.
- 1346 Murphy, J.B., Gutiérrez-Alonso, G., Nance, R.D., Fernández-Suárez, J., Keppie, J.D.,  
1347 Quesada, C. et al., 2006. Origin of the Rheic Ocean: rifting along a Neoproterozoic  
1348 suture? *Geology* 34, 325–328.
- 1349 Nance, R.D., Gutiérrez-Alonso, G., Keppie, J.D., Linnemann, U., Murphy, J.B.,  
1350 Quesada, C. et al., 2010. Evolution of the Rheic Ocean. *Gondwana Res.* 17, 194–  
1351 222.
- 1352 Navidad, M., Castiñeiras, P., 2011. Early Ordovician magmatism in the northern  
1353 Central Iberian Zone (Iberian Massif): new U–Pb (SHRIMP) ages and isotopic Sr–  
1354 Nd data. 11th ISOS, Alcalá de Henares, May 2011.



- 1355 Navidad, M., Castiñeiras, P., Casas, J.M., Liesa, M., Fernández-Suárez, J., Barnolas,  
1356 A., Carreras, J., Gil-Peña, I., 2010. Geochemical characterization and isotopic ages  
1357 of Caradocian magmatism in the northeastern Iberia: insights into the Late  
1358 Ordovician evolution of the northern Gondwana margin. *Gondwana Res.* 17, 325–  
1359 337.
- 1360 Navidad, M., Castiñeiras, P., Casas, J.M., Liesa, M., Belousova, E., Proenza, J.,  
1361 Aiglsperger, T., 2018. Ordovician magmatism in the Eastern Pyrenees: Implications  
1362 for the geodynamic evolution of northern Gondwana. *Lithos* 314–315, 479–496.
- 1363 Neiva, A.M.R., Williams, I.S., Ramos, J.M.F., Gomes, M.E.P., Silva, M.M.V.G.,  
1364 Antunes, I.M.H.R., 2009. Geochemical and isotopic constraints on the petrogenesis  
1365 of Early Ordovician granodiorite and Variscan two-mica granites from the Gouveia  
1366 area, central Portugal. *Lithos* 111, 186–202.
- 1367 Oggiano, G., Gaggero, L., Funedda, A., Buzzi, L., Tiepolo, M., 2010. Multiple early  
1368 Paleozoic volcanic events at the northern Gondwana margin: U–Pb age evidence  
1369 from the southern Variscan branch (Sardinia, Italy). *Gondwana Res.* 17, 44–58.
- 1370 Padel, M., Álvaro, J.J., Clausen, S., Guillot, F., Poujol, M., Chichorro, M., Monceret, E.,  
1371 Pereira, M.F., Vizcaíno, D., 2017. U–Pb laser ablation ICP–MS zircon dating across  
1372 the Ediacaran–Cambrian transition of the Montagne Noire, southern France. *C. R.  
1373 Geosci.* 349, 380–390.
- 1374 Padel, M., Clausen, S., Álvaro, J.J., Casas, J.M., 2018. Review of the Ediacaran–  
1375 Lower Ordovician (pre-Sardic) stratigraphic framework of the Eastern Pyrenees,  
1376 southwestern Europe. *Geol. Acta* 16, 339–355
- 1377 Palme, H., O'Neill, H.S.C., 2004. Cosmochemical estimates of mantle composition. In:  
1378 Treatise on Geochemistry 2 (Holland, H.D., Turekian, K.K., eds.), 1–38. Elsevier–  
1379 Pergamon, Oxford.
- 1380 Palmeri, R., Fanning, M., Franceschelli, M., Memmi, I., Ricci, C.A., 2004. SHRIMP  
1381 dating of zircons in eclogite from the Variscan basement in northeastern Sardinia  
1382 (Italy). *N. Jb. Miner., Mh.* 6, 275–288.



- 1383 Pankhurst, R.J., Rapela, C.W., Saavedra, J., Baldo, E., Dahlquist, J., Pascua, I.,  
1384 Fanning, C.M., 1998. The Famatinian magmatic arc in the central Sierras  
1385 Pampeanas, and Early to Middle Ordovician continental arc on the Gondwana  
1386 margin. In: The Proto-Andean Margin of Gondwana (Pankhurst, R.J., Rapela, C.E.,  
1387 eds.). Geol. Soc., London, Spec. Publ. 142, 343–367.
- 1388 Pavanello, P., Funedda, A., Northrup, C. J., Schmitz, M., Crowley, J., Loi, A., 2012.  
1389 Structure and U–Pb zircon geochronology in the Variscan foreland of SW Sardinia,  
1390 Italy. *Geol. J.* 47, 426–445.
- 1391 Pearce, J.A., 1996. Sources and settings of granitic rocks. *Episodes* 19, 120–125.
- 1392 Pearce, J.A., Harris, N.B.W., Tindle, A.G., 1984. Trace element discrimination  
1393 diagrams for the tectonic interpretation of granitic rocks. *J. Petrol.* 25, 956–983.
- 1394 Pereira, M.F., Solá, A.R., Chichorro, M., Lopes, L., Gerdes, A., Silva, J.B., 2012. North-  
1395 Gondwana assembly, break-up and paleogeography: U–Pb isotope evidence from  
1396 detrital and igneous zircons of Ediacaran and Cambrian rocks of SW Iberia.  
1397 *Gondwana Res.* 22(3–4), 866–881.
- 1398 Piercy, S.J., 2011. The setting, style, and role of magmatism in the formation of  
1399 volcanogenic massive sulphide deposits. *Miner. Deposita* 46, 449–471.
- 1400 Pistis, M., Loi, A., Dabard, M.P., 2016. Influence of relative sea-level variations on the  
1401 genesis of palaeoplacers, the examples of Sarrabus (Sardinia, Italy) and the  
1402 Armorican Massif (western France). *C. R. Geosci.* 348(2), 150–157.
- 1403 Pillola, G.L., Leone, F., Loi, A., 1998. The Cambrian and Early Ordovician of SW  
1404 Sardinia. *Gior. Geol. (ser. 3)*, Spec. Iss. 60, 25–38.
- 1405 Pitra, P., Poujol, M., Den Driessche, J.V., Poilvet, J. C., Paquette, J.L., 2012. Early  
1406 Permian extensional shearing of an Ordovician granite: the Saint-Eutrope “C/S-like”  
1407 orthogneiss (Montagne Noire, French Massif Central). *C. R. Geosci.* 344, 377–384.
- 1408 Pouclet, A., Álvaro, J.J., Bardintzeff, J.M., Gil Imaz, A., Monceret, E., Vizcaíno D.,  
1409 2017. Cambrian–Early Ordovician volcanism across the South Armorican and



- 1410 Occitan Domains of the Variscan Belt in France: Continental break-up and rifting of  
1411 the northern Gondwana margin. *Geosci. Frontiers* 8, 25–64.
- 1412 Puddu, C., Álvaro J.J., Casas, J.M., 2018. The Sardic unconformity and the Upper  
1413 Ordovician successions of the Ribes de Freser area, Eastern Pyrenees. *J. Iberian  
1414 Geol.* 44, 603–617.
- 1415 Puddu, C., Álvaro, J.J., Carrera, N., Casas, J.M., 2019. Deciphering the Sardic  
1416 (Ordovician) and Variscan deformations in the Eastern Pyrenees. *J. Geol. Soc.*  
1417 176(6), 1191–1206.
- 1418 Quesada, C., 1991. Geological constraints on the Paleozoic tectonic evolution of  
1419 tectonostratigraphic terranes in the Iberian Massif. *Tectonophysics* 185, 225–245.
- 1420 Rabin, M., Trap, P., Carry, N. Fréville, K. Cenki-Tok, B. Lobjoie, C. Gonçalves, P.,  
1421 Marquer, D., 2015. Strain partitioning along the anatetic front in the Variscan  
1422 Montagne Noire massif (southern French Massif Central). *Tectonics* 34, 1709–1735.
- 1423 Robert, J. F. 1980. Étude géologique et métallogénique du val de Ribas sur le versant  
1424 espagnol des Pyrénées catalanes. PhD, Univ. Franche-Comté.
- 1425 Robert, J.F., Thiebaut, J., 1976. Découverte d'un volcanisme acide dans le Caradoc de  
1426 la région de Ribes de Freser (Prov. de Gérone). *C. R. Acad. Sci., Paris* 282, 2050–  
1427 2079.
- 1428 Roger, F., Respaut, J.P., Brunel, M., Matte, Ph., Paquette, J.L., 2004. Première  
1429 datation U–Pb des orthogneiss oeillés de la zone axiale de la Montagne Noire (Sud  
1430 du Massif central): nouveaux témoins du magmatisme ordovicien dans la chaîne  
1431 varisque. *C. R. Geosci.* 336, 19–28
- 1432 Roger, F., Teyssier, C., Respaut, J.P., Rey, P.F., Jolivet, M., Whitney, D.L., Paquette,  
1433 J.L., Brunel, M., 2015. Timing of formation and exhumation of the Montagne Noire  
1434 double dome, French massif Central. *Tectonophysics* 640–641, 53–69.
- 1435 Rollison, H.R., 1993. *Using Geochemical Data: Evaluation, Presentation, Interpretation*.  
1436 Longman Group, London, 352 p.



- 1437 Romão, J., Dunning, G., Marcos, A., Dias, R., Ribeiro, A., 2010. O lacólito granítico de  
1438 Mação-Penhascoso: idade e as suas implicações (SW da Zona Centro-Ibérica). *e-*  
1439 *Terra* 16, 1–4.
- 1440 Rossi, P., Oggiano, G., Cocherie, A., 2009. A restored section of the “southern  
1441 Variscan realm” across the Corsica-Sardinia microcontinent. *C. R. Geosci.* 34, 224–  
1442 238.
- 1443 Rubio-Ordóñez, A., Valverde-Vaquero, P., Corretgé, L. G., Cuesta-Fernández, A.,  
1444 Gallastegui, G., Fernández-González, M., Gerdes, A., 2012. An Early Ordovician  
1445 tonalitic-granodioritic belt along the Schistose-Greywacke Domain of the Central  
1446 Iberian Zone (Iberian Massif, Variscan Belt). *Geol. Mag.* 149, 927–939.
- 1447 Rudnick, R.L., Gao, S., 2003. Composition of the Continental Crust. In: *Treatise on*  
1448 *Geochemistry* (Holland, H.D., Turekian, K.K., eds.), vol. 3, 1–64. Elsevier-  
1449 Pergamon, Oxford.
- 1450 Sánchez-García, T., Bellido, F., Quesada, C., 2003. Geodynamic setting and  
1451 geochemical signatures of Cambrian–Ordovician rift-related igneous rocks (Ossa-  
1452 Morena Zone, SW Iberia). *Tectonophysics* 365, 233–255.
- 1453 Sánchez-García, T., Quesada, C., Bellido, F., Dunning, G., González de Tánago, J.,  
1454 2008. Two-step magma flooding of the upper crust during rifting: the Early Paleozoic  
1455 of the Ossa-Morena Zone (SW Iberia). *Tectonophysics* 461, 72–90.
- 1456 Sánchez-García, T., Bellido, F., Pereira, M.F., Chichorro, M., Quesada, C., Pin, Ch.,  
1457 Silva, J.B., 2010. Rift-related volcanism predating the birth of the Rheic Ocean  
1458 (Ossa-Morena zone, SW Iberia). *Gondwana Res.* 17, 392–407.
- 1459 Sánchez-García, T., Quesada, C., Bellido, F., Dunning, G.R., Pin, Ch., Moreno-Eiris,  
1460 E., Perejón, A., 2016. Age and characteristics of the Loma del Aire unit (SW Iberia):  
1461 Implications for the regional correlation of the Ossa-Morena Zone. *Tectonophysics*  
1462 681, 58–72.
- 1463 Sánchez-García, T., Chichorro, M., Solá, R., Álvaro, J.J., Díez Montes, A., Bellido, F. et  
1464 al. 2019. The Cambrian–Early Ordovician Rift Stage in the Gondwanan Units of the



- 1465 Iberian Massif. In: *The Geology of Iberia: A Geodynamic Approach* (Quesada, C.,  
1466 Oliveira, J.T., eds.). *Regional Geol. Rev.* 1, 27–74.
- 1467 Schaltegger, U., Abrecht, J., Corfu, F., 2003. The Ordovician orogeny in the Alpine  
1468 basement: constraints from geochronology and geochemistry in the Aar Massif  
1469 (Central Alps). *Schweizerische Miner. Petrogr. Mitteil.* 83, 183–195.
- 1470 Shaw, J., Johnston, S., Gutiérrez-Alonso, G., Weil, A.B., 2012. Oroclines of the  
1471 Variscan orogen of Iberia: paleocurrent analysis and paleogeographic implications.  
1472 *Earth Planet. Sci. Lett.* 329–330, 60–70.
- 1473 Shaw, J., Gutiérrez-Alonso, G., Johnston, S., Pastor Galán, D., 2014. Provenance  
1474 variability along the early Ordovician north Gondwana margin: paleogeographic and  
1475 tectonic implications of U–Pb detrital zircon ages from the Armorican Quartzite of  
1476 the Iberian Variscan belt. *Geol. Soc. Am. Bull.* 126(5–6), 702–719.
- 1477 Solá, A.R., 2007. Relações Petrogeoquímicas dos Maciços Graníticos do NE  
1478 Alentejano. PhD, Univ. Coimbra.
- 1479 Solá, A.R., Pereira, M.F., Williams, I.S., Ribeiro, M.L., Neiva, A.M.R., Montero, P., Bea,  
1480 F., Zinger, T., 2008. New insights from U–Pb zircon dating of Early Ordovician  
1481 magmatism on the northern Gondwana margin: the Urra formation (SW Iberian  
1482 Massif, Portugal). *Tectonophysics* 461, 114–129.
- 1483 Stille, H., 1939. Bemerkungen betreffend die "Sardische" Faultung und den Ausdruck  
1484 "Ophiolitisch". *Zeits. Deuts. Gess. Geowiss.* 91, 771–773.
- 1485 Sun, S.S., McDonough, W.F., 1989. Chemical and isotopic systematics of oceanic  
1486 basalts: implications for mantle composition and processes. In: *Magmatism in the*  
1487 *Ocean Basins* (Saunders, A.D., Norry, M.J., eds.). *Geol. Soc., Spec. Publ.* 42, 13–  
1488 345.
- 1489 Syme, E.C., 1998. Ore-Associated and Barren Rhyolites in the central Flin Flon Belt:  
1490 Case Study of the Flin Flon Mine Sequence. Manitoba Energy and Mines, Open File  
1491 Report OF98–9, 1–32



- 1492 Talavera, C., 2009. Pre-Variscan magmatism of the Central Iberian Zone: chemical  
1493 and isotope composition, geochronology and geodynamic significance. PhD, Univ.  
1494 Granada.
- 1495 Talavera, C., Bea F, Montero P., Whitehouse, M., 2008. A revised Ordovician age for  
1496 the Sisargas orthogneiss, Galicia (Spain). Zircon U–Pb ion-microprobe and LA–  
1497 ICPMS dating. *Geol. Acta* 8, 313–317.
- 1498 Talavera, C., Montero, P., Bea, F., González Lodeiro, F., Whitehouse, M., 2013. U–Pb  
1499 Zircon geochronology of the Cambro–Ordovician metagranites and metavolcanic  
1500 rocks of central and NW Iberia. *Int. J. Earth. Sci.* 102, 1–23.
- 1501 Taylor, S.R., McLennan, S.M., 1985. *The Continental Crust: Its Composition and*  
1502 *Evolution.* Blackwell, London, 312 pp.
- 1503 Teichmüller, R., 1931. Zur Geologie des Thyrrhenisgebietes, Teil 1: Alte und junge  
1504 Krustenbewegungen im südlichen Sardinien. *Abh. Der wissen. Gess. Göttingen*  
1505 (Math.-Phys. Kl) 3, 857–950.
- 1506 Teipel, U., Eichhorn, R., Loth, G., Rohrmüller, J., Höll, R., Kennedy, A., 2004. U–Pb  
1507 SHRIMP and Nd isotopic data from the western Bohemian Massif (Bayerischer  
1508 Wald, Germany): Implications for Upper Vendian and Lower Ordovician magmatism.  
1509 *Int. J. Earth Sci.* 93, 782–801.
- 1510 Thompsom, M.D., Grunow, A.M., Ramezani, J., 2010. Cambro–Ordovician  
1511 paleogeography of the Southeastern New England Avalon Zone: Implications for  
1512 Gondwana breakup. *Geol. Soc. Am. Bull.* 122, 76–88.
- 1513 Tichomirowa, M., Berger, H.J., Koch, E.A., Belyatski, B., Götze, J., Kempe, U.,  
1514 Nasdala, L., Schaltegger, U., 2001. Zircon ages of high-grade gneisses in the  
1515 Eastern Erzgebirge (Central European Variscides) – constraints on origin of the  
1516 rocks and Precambrian to Ordovician magmatic events in the Variscan foldbelt.  
1517 *Lithos* 56, 303–332.
- 1518 Tichomirowa, M., Sergeev, S., Berger, H.J., Leonhardt, D., 2012. Inferring protoliths of  
1519 high-grade metamorphic gneisses of the Erzgebirge using zirconology,



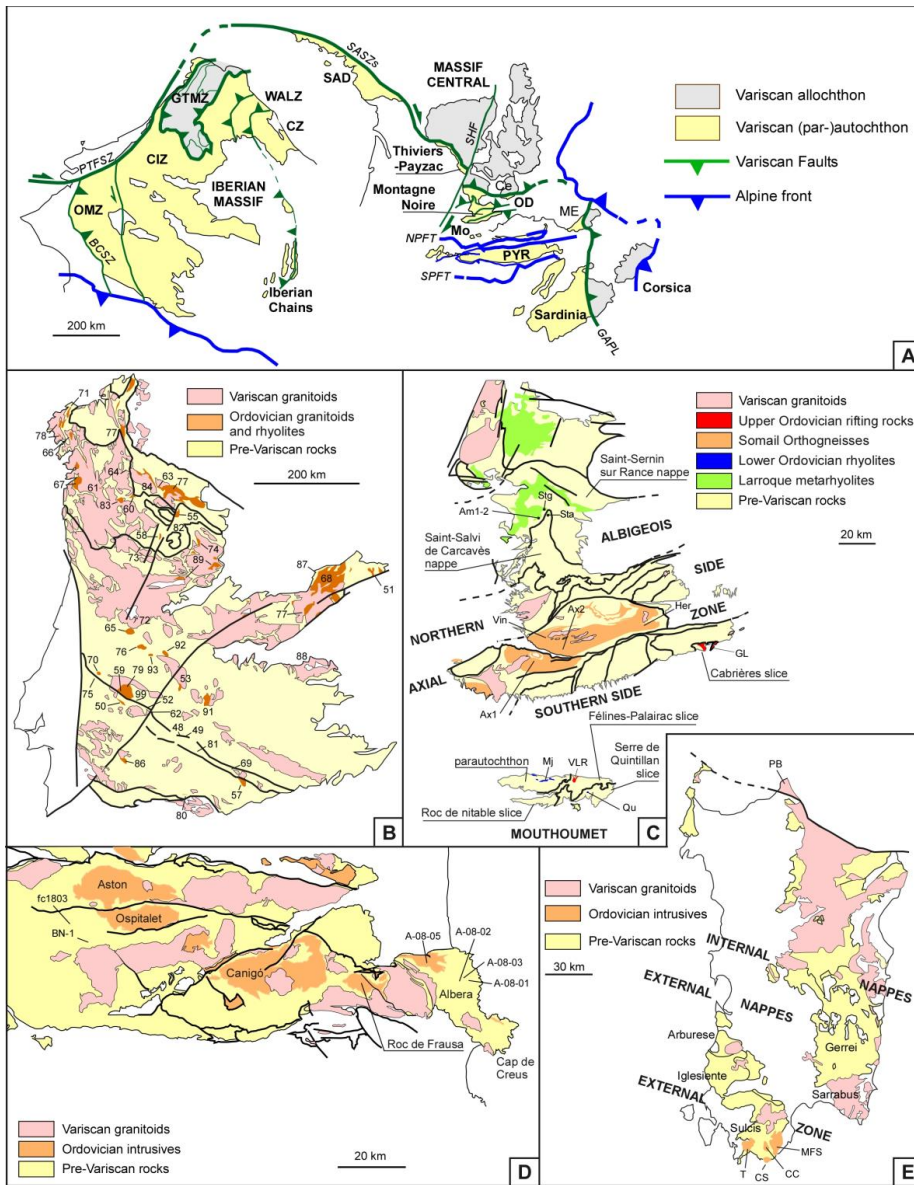
- 1520 geochemistry and comparison with lower-grade rocks from Lusatia (Saxothuringia,  
1521 Germany). *Contrib. Mineral. Petrol.* 164, 375–396.
- 1522 Valverde-Vaquero, P., Dunning, G.R., 2000. New U–Pb ages for Early Ordovician  
1523 magmatism in Central Spain. *J. Geol. Soc. London* 157, 15–26.
- 1524 Valverde-Vaquero, P., Marcos, A., Farias, P., Gallastegui, G., 2005. U–Pb dating of  
1525 Ordovician felsic volcanism in the Schistose Domain of the Galicia-Trás-os-Montes  
1526 Zone near Cabo Ortegal (NW Spain). *Geol. Acta* 3, 27–37.
- 1527 Valverde-Vaquero, P., Farias, P., Marcos, A., Gallastegui, G., 2007. U–Pb dating of  
1528 Siluro–Ordovician volcanism in the Verín synform (Orense, Schistose Domain,  
1529 Galicia-Trás-os-montes Zone). *Geogaceta* 41, 247–250.
- 1530 Vilà, M., Pin, C., Enrique, P., Liesa, M., 2005. Telescoping of three distinct magmatic  
1531 suites in an orogenic setting: Generation of Hercynian igneous rocks of the Albera  
1532 Massif (Eastern Pyrenees). *Lithos* 83, 97–127.
- 1533 Villaseca, C., Castiñeiras, P., Orejana, D., 2013. Early Ordovician metabasites from the  
1534 Spanish Central System: A remnant of intraplate HP rocks in the Central Iberian  
1535 Zone. *Gondwana Res.* 27, 392–409.
- 1536 Villaseca, C., Merino Martínez, E., Orejana, D., Andersen, T., Belousova, E., 2016.  
1537 Zircon Hf signatures from granitic orthogneisses of the Spanish Central System:  
1538 Significance and sources of the Cambro–Ordovician magmatism in the Iberian  
1539 Variscan Belt. *Gondwana Res.* 34, 60–83.
- 1540 Von Quadt, A., 1997. U–Pb zircon and Sr–Nd–Pb whole-rock investigations from the  
1541 continental deep drilling (KTB). *Geol. Rundsch.* 86 (suppl.), S258–S271.
- 1542 Von Raumer, J.F., Stampfli, G.M., 2008. The birth of the Rheic Ocean – early  
1543 Palaeozoic subsidence patterns and tectonic plate scenarios. *Tectonophysics* 461,  
1544 9–20.
- 1545 Von Raumer, J.F., Stampfli, G.M., Borel, G., Bussy, F., 2002. The organization of pre–  
1546 Variscan basement areas at the Gondwana margin. *Int. J. Earth Sci.* 91, 35–52.



- 1547 Von Raumer, J.F., Bussy, F., Schaltegger, U., Schulz, B., Stampfli, G., 2013. Pre-  
1548 Mesozoic Alpine basements: their place in the European Paleozoic framework.  
1549 Geol. Soc. Am. Bull. 125, 89–108.
- 1550 Von Raumer, J.F., Stampfli, G.M., Arenas, R., Sánchez Martínez, S., 2015. Ediacaran  
1551 to Cambrian oceanic rocks of the Gondwanan margin and their tectonic  
1552 interpretation. Int. J. Earth Sci. 104, 1107–1121.
- 1553 Whalen, J.B., Currie, K.L., Chappell, B.W., 1987. A-type granites: Geochemical  
1554 characteristics, discrimination and petrogenesis. Contr. Miner. Petrol. 95, 407–419.
- 1555 Winchester, J.A., Floyd, P.A., 1977. Geochemical discrimination of different magma  
1556 series and their differentiation products using immobile elements. Chem. Geol. 20,  
1557 325–343.
- 1558 Zeck, H.P., Whitehouse, M.J., Ugidos, J.M., 2007.  $496 \pm 3$  Ma zircon ion microprobe  
1559 age for pre-Hercynian granite, Central Iberian Zone, NE Portugal (earlier claimed  
1560  $618 \pm 9$  Ma). Geol. Mag. 144, 21–31.
- 1561 Zurbriggen, R., 2015. Ordovician orogeny in the Alps – a reappraisal. Int. J. Earth Sci.  
1562 104, 335–350.
- 1563 Zurbriggen, R., 2017. The Cenerian orogeny (early Paleozoic) from the perspective of  
1564 the Alpine region. Int. J. Earth Sci. 106, 517–529.
- 1565 Zurbriggen, R., Franz, L., Handy, M.R., 1997. Pre-Variscan deformation,  
1566 metamorphism and magmatism in the Strona-Ceneri Zone (southern Alps of  
1567 northern Italy and southern Switzerland). Schweiz. Miner. Petrograph. Mitteil. 77,  
1568 361–380.
- 1569



1570 FIGURES

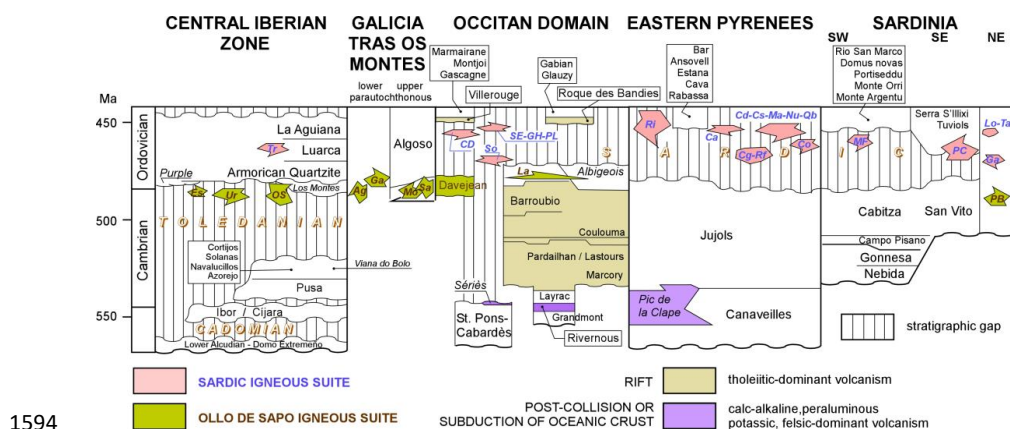


1571

1572 **Figure 1.** A. Reconstruction of the south-western European margin of Gondwana in  
 1573 Late Carboniferous–Early Permian times; modified from Pouclet et al. (2017). B.  
 1574 Setting of samples in the Central Iberian and Galicia-Trás-os-Montes zones; 48-  
 1575 Aceuchal, 49- Almendralejo, 50-Alter do Chao-Alter Pedroso, 51-Antoñita, 52-



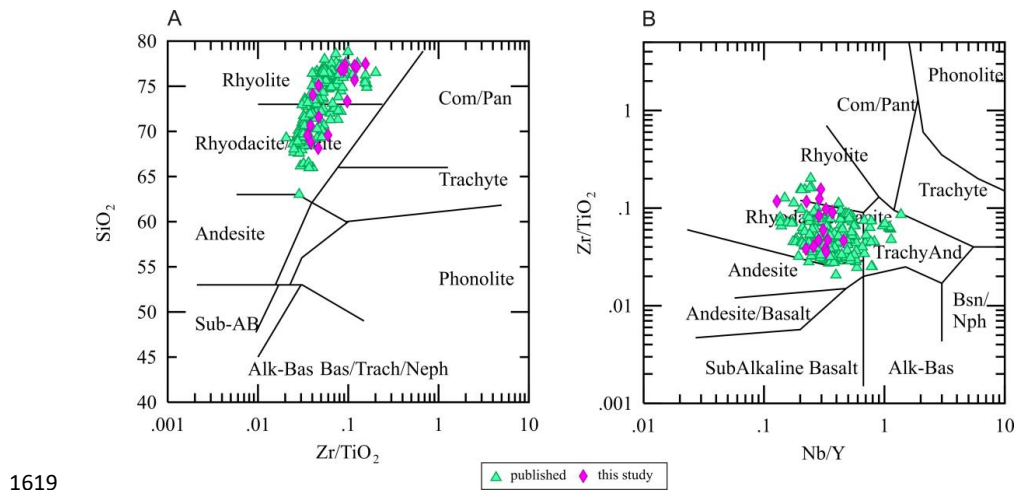
1576 Arronches, 53- Arroyo de la Luz, 55- Bragança, 57- Cardenchoosa, 58 -Carrapatas,  
1577 Facho & Valbenfeito, 59- Carrascal, 60- Carraxo, 61- Celanova-Bande, 62- Cevadais,  
1578 63- Covelo, 64- Os los Peares, 65- Fundao, 66- Galicia orthogneiss, 69- Las Minillas,  
1579 70- Maçao, 71- Malpica, 72- Manteigas, 73- Marão-Eucisia-Moncorvo, 74- Miranda do  
1580 Douro, 75- Mouriscas, 76- Oledo, 77- Ollo de Sapo, 78- Pontevedra-Sisargas, 79-  
1581 Portalegre, 80- Ribera deHuelva, 81- Rivera del Fresno, 82- Saldanha, 83- San  
1582 Mamede, 84-San Sebastián, 86- São Marcos do Campo, 87-Tenzuela, 88- Toledo  
1583 (Anatetic Dome), 89- Tormes Dome, 90- Urra, 91- Zarza de Montanchez 92- Zarza la  
1584 Mayor and 93- Zebreira; modified from Sánchez-García et al. (2019). C. Setting of  
1585 samples in the Montagne Noire and Mouthoumet massifs; Am1-2 Larroque hamlet  
1586 (Ambialet), Stg- St.Géraud Sta- St. André, Mj- Montjoi, Qu- Quintillan, GL- Roque de  
1587 Bandies, VLR- Villerouge-Termenès, VIN- Le Vintrou, HER- Gorges d'Héric (Caroux  
1588 massif), Ax1- S Mazamet (Nore massif), Ax2 (Rou)- S Rouayroux (Agout massif);  
1589 modified from Álvaro et al. (2016). D. Setting of Pyrenean samples; modified from  
1590 Casas et al. (2019). E. Setting of Sardinian samples; CS 2,3,4,8- Spartivento Cap, T2-  
1591 Tuerreda, CC5- Cuile Culurgioni, MF1- Monte Filau, MFS1-Monte Settiballas, PB-  
1592 Punta Bianca; modified from Oggiano et al. (2010).  
1593



1594 **Figure 2.** Stratigraphic comparison of the Cambro-Ordovician successions from the  
 1595 Central Iberian Zone, Galicia Trás-os-Montes Zone, Occitan Domain, Eastern  
 1596 Pyrenees and Sardinia; modified from Álvaro et al. (2014b, 2016, 2018), Pouplet et al.  
 1597 (2017) and Sánchez-García et al. (2019); abbreviations: Ca Campelles ignimbrites (ca.  
 1598 455 Ma, Martí et al., 2014), CD Cadí gneiss ( $456 \pm 5$  Ma, Casas et al., 2010), Cg  
 1599 Canigó gneiss (472–462 Ma, Cocherie et al., 2005; Navidad et al., 2018), Co Cortalets  
 1600 metabasite ( $460 \pm 3$  Ma, Navidad et al., 2018), Cs Casemí gneiss (446  $\pm 5$  and  $452 \pm 5$   
 1601 Ma, Casas et al., 2010), Es Estremoz rhyolites (499 Ma, Pereira et al., 2012), Ga Golfo  
 1602 Aranci orthogneiss ( $469 \pm 3.7$  Ma, Giacomini et al., 2006), GH Gorges d'Heric  
 1603 orthogneiss ( $450 \pm 6$  Ma, Roger et al., 2004), La Larroque Volcanic Complex, Ma  
 1604 Marialettes microdiorite ( $453 \pm 4$  Ma, Casas et al., 2010), Lo Lodè orthogneiss ( $456 \pm 14$   
 1605 Ma, Helbing and Tiepolo, 2005), MF Monte Filau-Capo Spartivento orthogneiss ( $449 \pm$   
 1606 6 Ma, Ludwing and Turi, 1989;  $457.5 \pm 0.3$  and  $458.2 \pm 0.3$  Ma, Pavanello et al., 2012),  
 1607 Nu Núria gneiss ( $457 \pm 4$  Ma, Martínez et al., 2011), OS Ollo de Sapo rhyolites and  
 1608 ash-fall tuff beds (ca. 477 Ma, Gutiérrez-Alonso et al., 2016), PL Pont de Larn  
 1609 orthogneiss ( $456 \pm 3$  Ma, Roger et al., 2004), Qb Queralbs gneiss ( $457 \pm 5$  Ma,  
 1610 Martínez et al., 2011), PB Punta Bianca orthogneiss (broadly Furongian–Tremadocian  
 1611 in age), PC Porto Corallo dacites ( $465.4 \pm 1.9$  and  $464 \pm 1$  Ma, Giacomini et al., 2006;  
 1612 Oggiano et al., 2010), Ri Ribes granophyre ( $458 \pm 3$  Ma, Martínez et al., 2011), Rf Roc



- 1614 de Frausa gneiss ( $477 \pm 4$ ,  $476 \pm 5$  Ma, Cocherie et al., 2005; Castiñeiras et al., 2008),  
1615 So Somain orthogneiss ( $471 \pm 4$  Ma, Cocherie et al. 2005), SE Saint Eutrope gneiss  
1616 ( $455 \pm 2$  Ma, Pitra et al., 2012), Ta Tanaunella orthogneiss  $458 \pm 7$  Ma (Helbing and  
1617 Tiepolo, 2005), Tr Turchas and Ur Urra rhyolites.  
1618

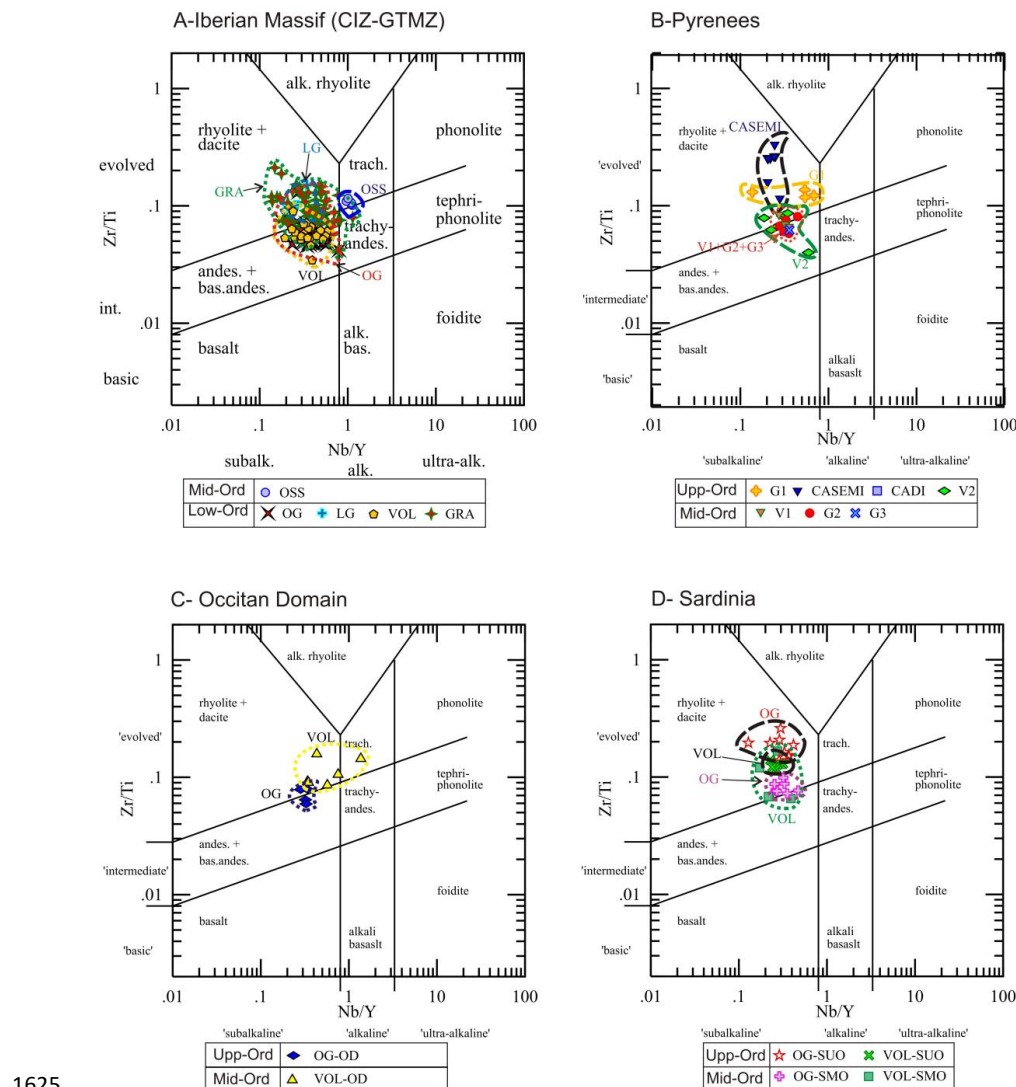


1619

1620

1621 **Figure 3.  $\text{SiO}_2$  vs.  $\text{Zr}/\text{TiO}_2$  and  $\text{Zr}/\text{TiO}_2$  vs.  $\text{Nb}/\text{Y}$  plots (Winchester and Floyd, 1977)**  
1622 **showing the composition of new samples (purple diamonds) and those taken**  
1623 **from the literature (green triangles).**

1624

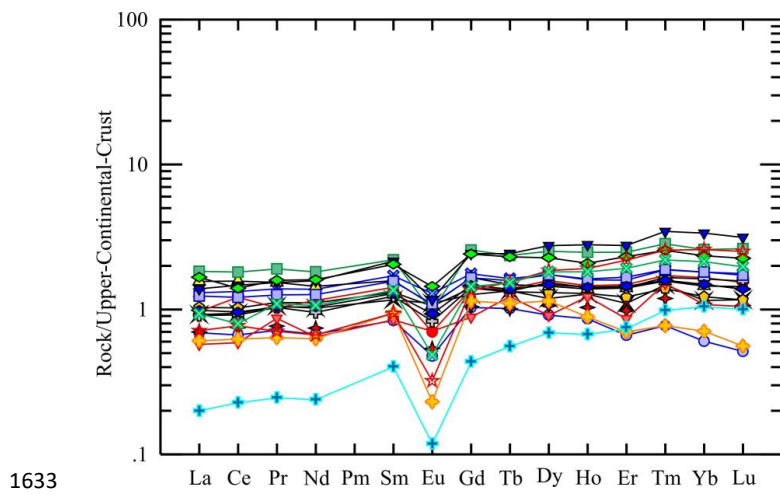


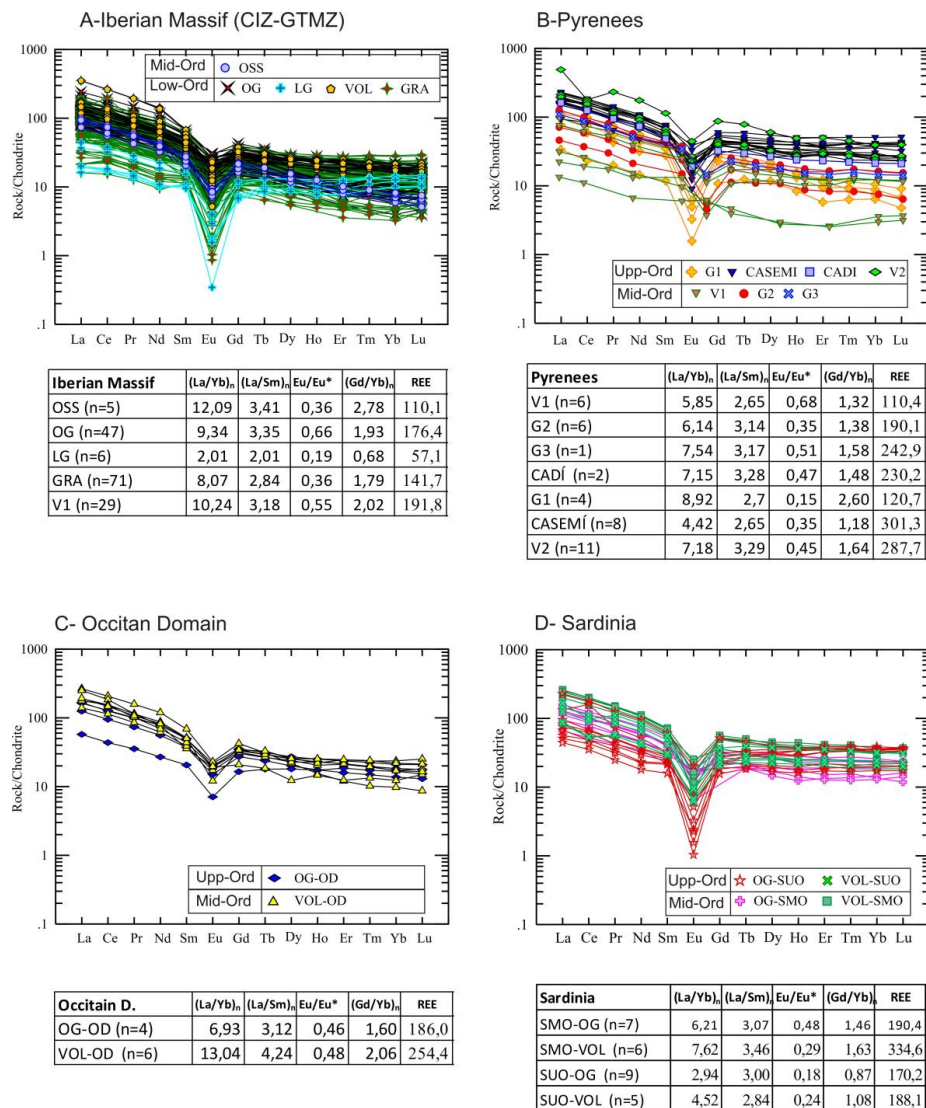
1625

1626

1627 **Figure 4. Zr/Ti vs. Nb/Y discrimination diagram (after Winchester and Floyd,  
 1628 1977; Pearce, 1996). A. Lower–Middle Ordovician rocks of Iberian Massif (Central  
 1629 Iberian and Galicia-Trás-os-Montes zones). B. Middle–Upper Ordovician rocks of  
 1630 the eastern Pyrenees. C) Middle Ordovician rocks of the Occitan Domain. C–D.  
 1631 Middle–Upper Ordovician rocks of Sardinia.**

1632

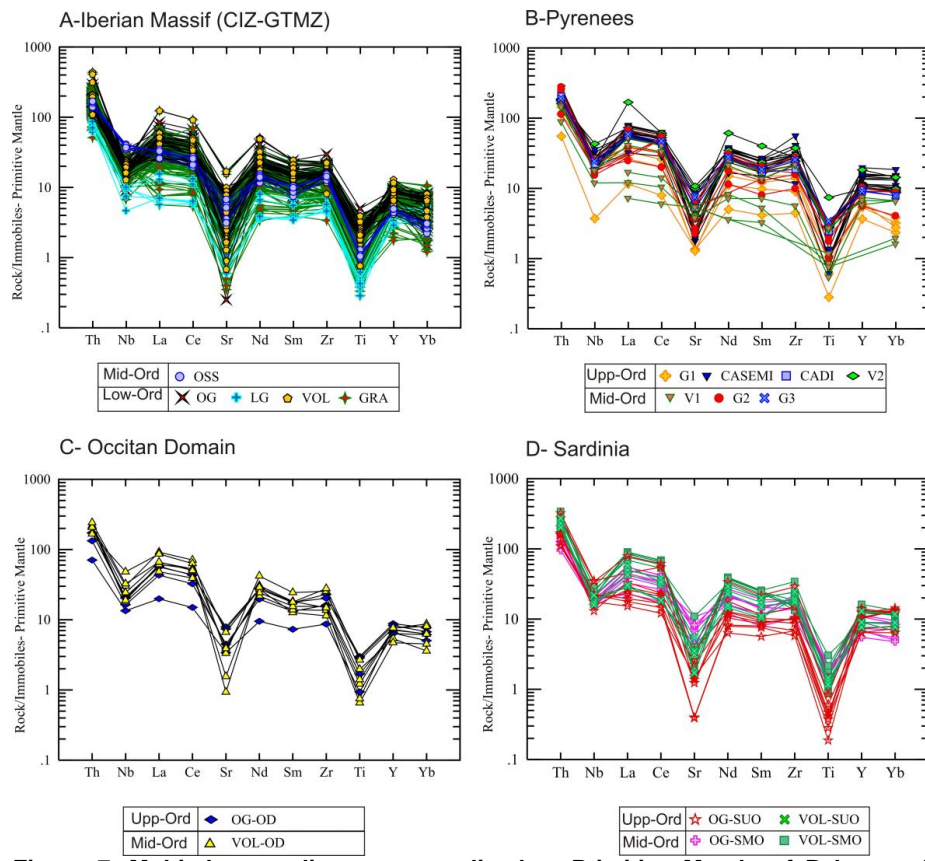




1637

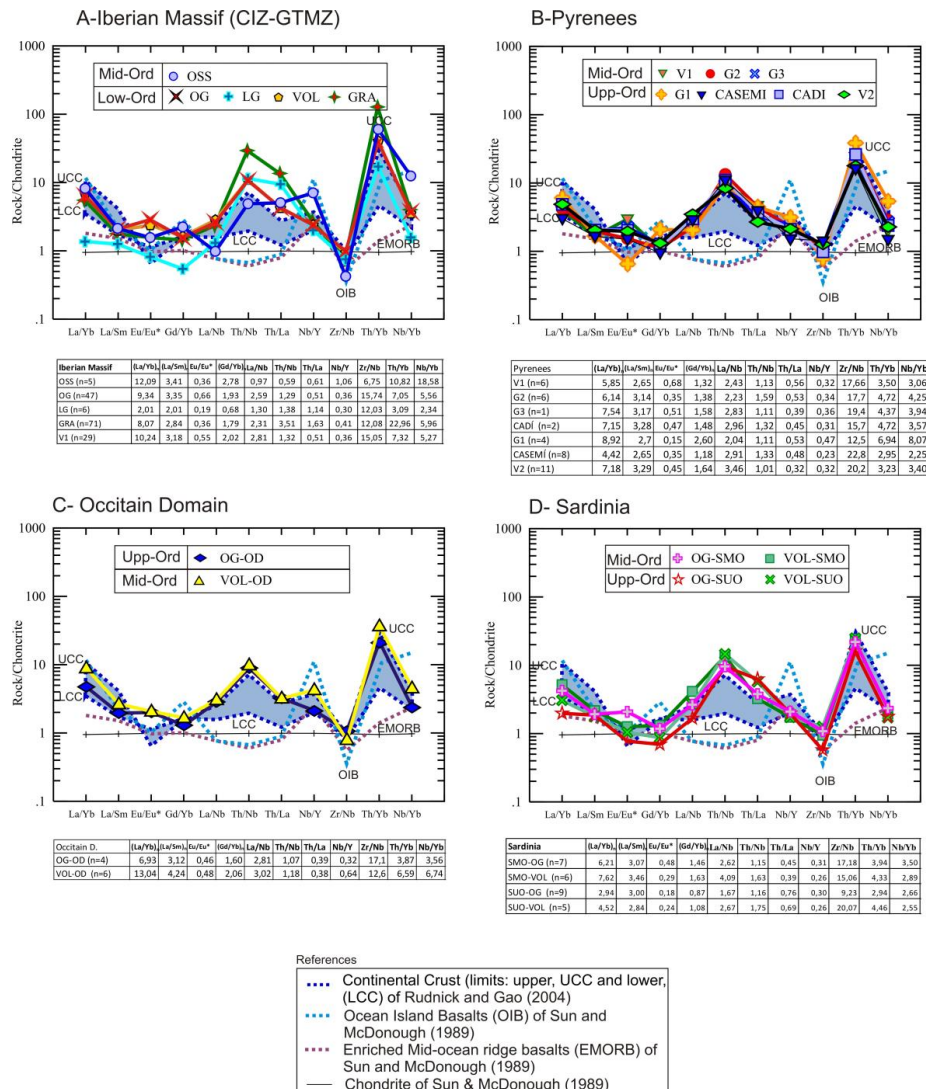
1638 **Figure 6. Chondrite-normalized REE patterns (Sun and McDonough, 1989) for all**  
 1639 **study samples.**

1640



1641  
 1642 **Figure 7. Multi-element diagram normalised to Primitive Mantle of Palme and**  
 1643 **O'Neill (2004) for all study samples.**

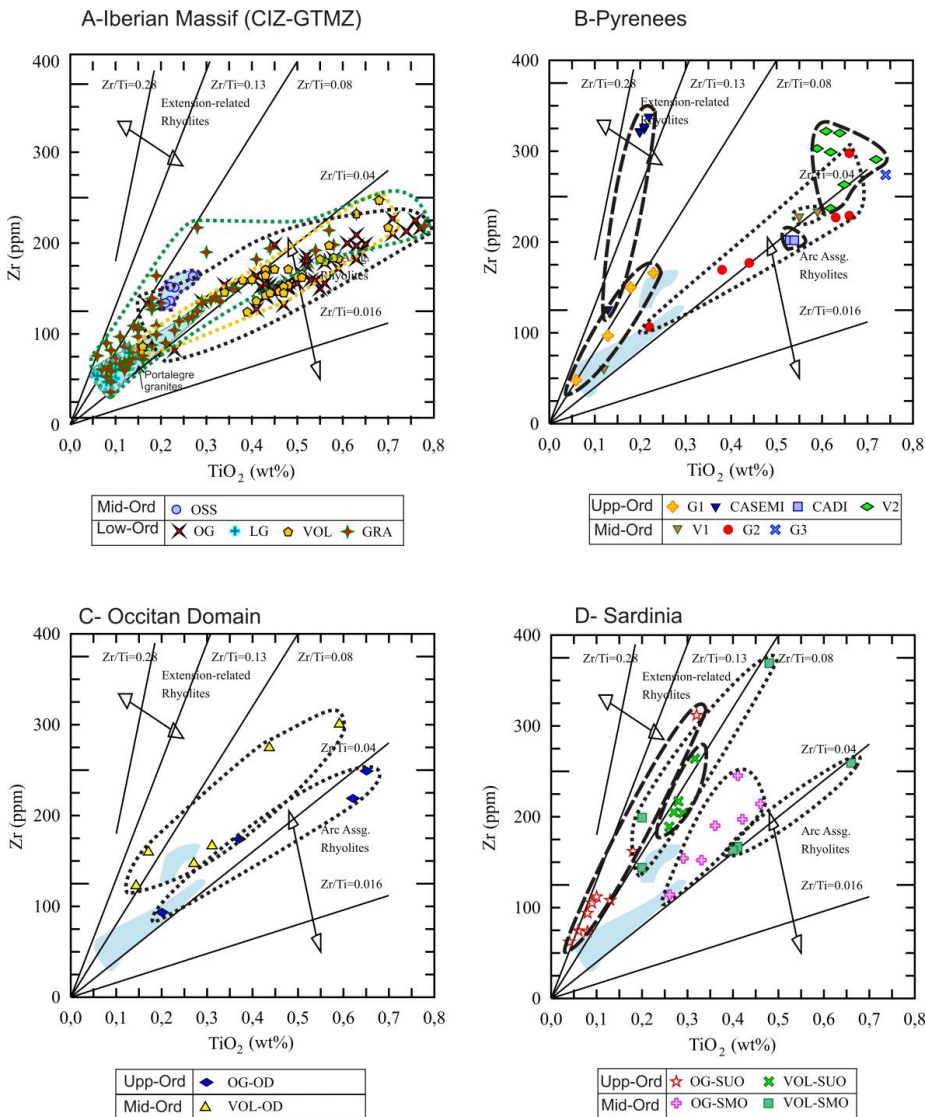
1644



1645

1646 **Figure 8. Chondrite-normalised isotope ratio patterns (Sun and McDonough,**  
 1647 **1989) for standard comparison for all study samples. Blue area: limits of**  
 1648 **continental crustal values (Lower and Upper) of Rudnick and Gao (2003).**

1649

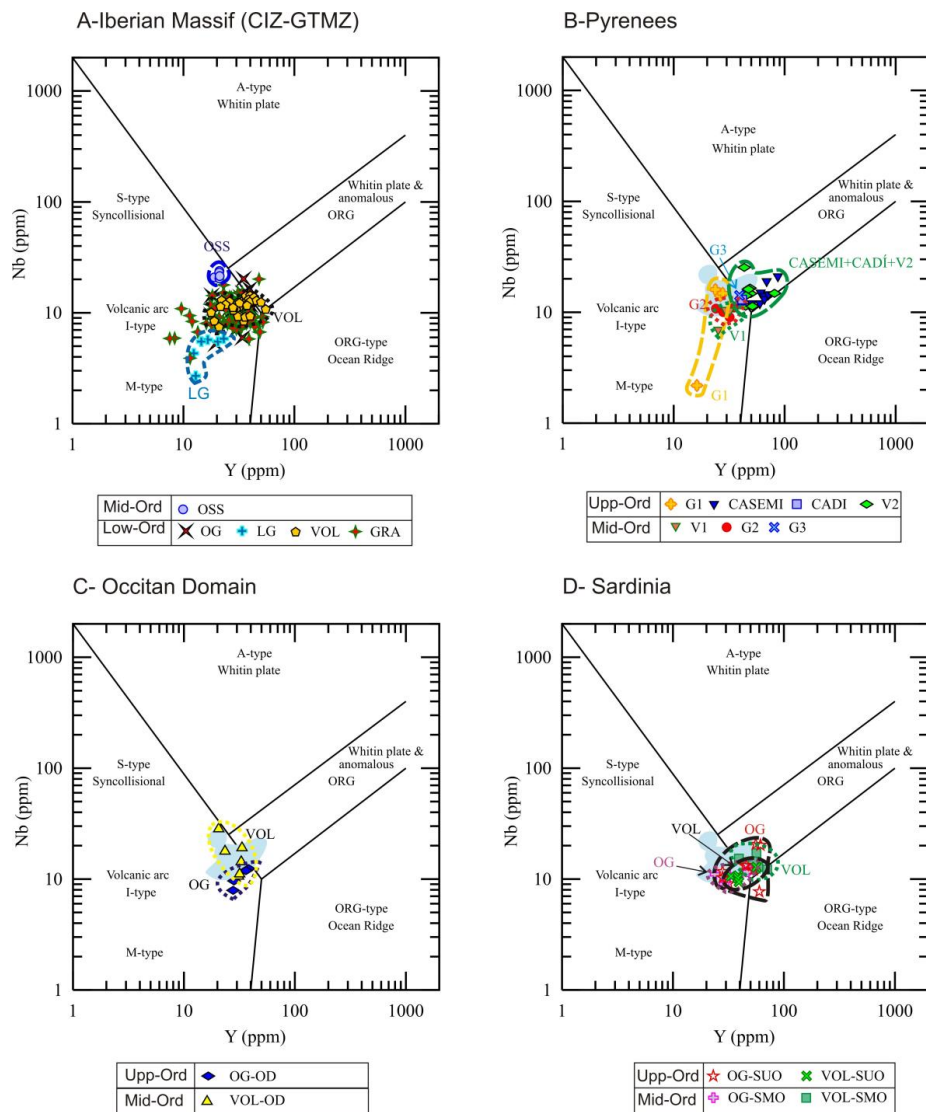


1650

1651 **Figure 9. Tectonic discriminating diagram of Zr vs. TiO<sub>2</sub> (Syme, 1998) for all study**

1652 **samples.**

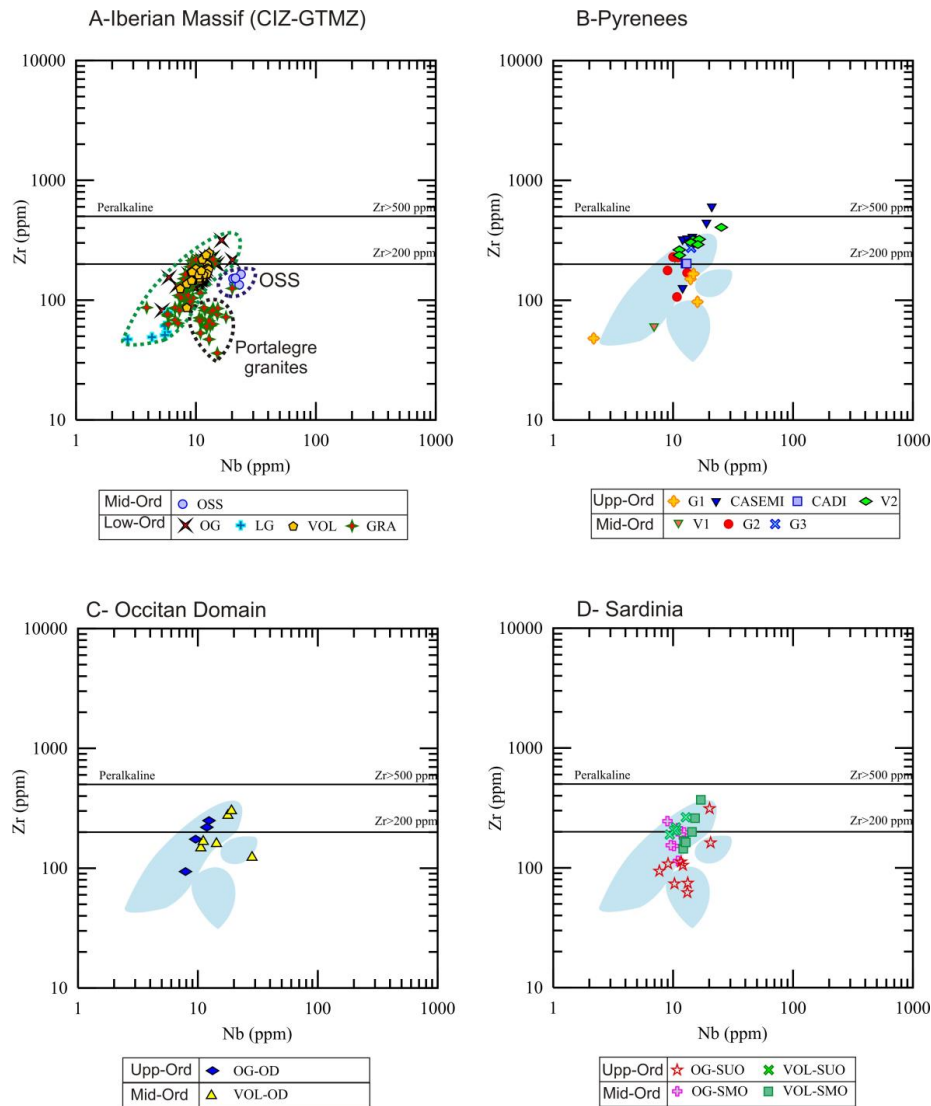
1653



1654

1655 **Figure 10. Tectonic discriminating diagram of Y vs. Nb (Pearce et al., 1984) for all**  
 1656 **study samples.**

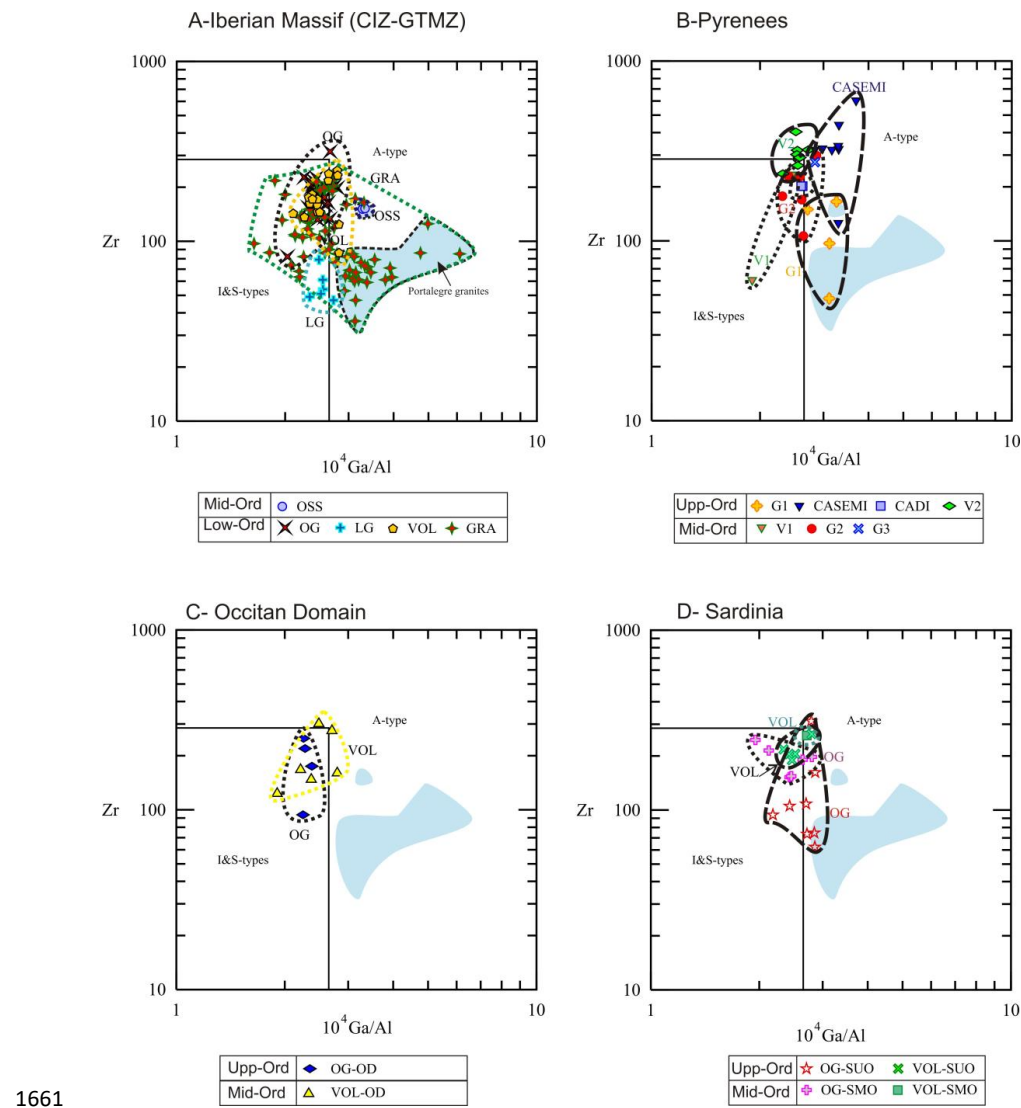
1657



1658

1659 **Figure 11. Zr vs.  $10^4$  Ga/Al discrimination diagram (Whalen et al., 1987).**

1660

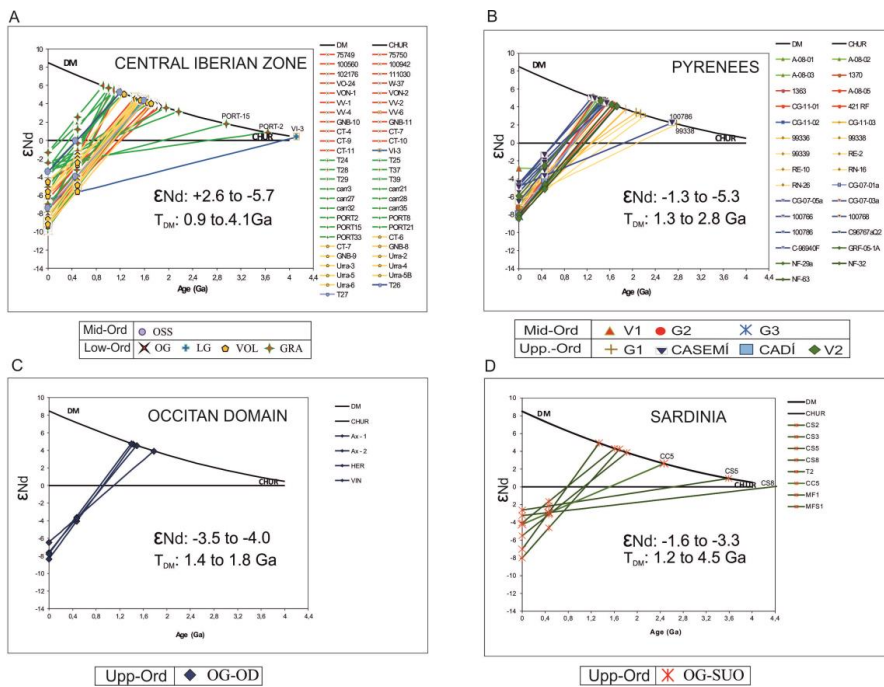


1661

1662 **Figure 12.** Zr–Nb plot diagram (Leat et al., 1986; modified by Piercy, 2011) for all

1663 study samples.

1664



1665

1666 Figure 13.  $\epsilon_{\text{Nd}}(t)$  vs. age diagram (DePaolo and Wasserburg, 1976; DePaolo, 1981)

1667 for study sampled. A. Central Iberian and Galicia-Trás-os-Montes Zones. B.

1668 Eastern Pyrenees. C. Occitan Domain. D. Sardinia; see references in the text.

1669



1670 TABLES

Sample	PYRENEES			MONTAGNE NOIRE				SARDINIA									
	Albera	Pallares	Andorra	Axial	Zone			Extrema	Zone	Inner	Zone	T2	PB50	PB100			
A-08-03	fc1803	BN 1		Ax - 1	Ax - 2	HER	VIN	CC 5	CS 2	CS 3	CS 5	CS 8	MF 1	MFS 1	T 2	PB50	PB100
<b>SiO<sub>2</sub></b>	68.38	71.67	69.18	70.38	67.43	68.31	73.97	76.43	75.14	76.52	76.61	76.36	72.13	75.94	75.55	68.93	67.24
<b>TiO<sub>2</sub></b>	0.57	0.63	0.61	0.36	0.64	0.61	0.20	0.08	0.08	0.09	0.04	0.06	0.31	0.13	0.18	0.41	0.46
<b>Al<sub>2</sub>O<sub>3</sub></b>	15.68	14.24	15.05	14.90	15.76	15.39	13.82	13.28	12.81	11.80	12.71	12.63	13.80	13.16	12.94	16.32	15.79
<b>Fe<sub>2</sub>O<sub>3</sub></b>	4.09	4.54	4.20	3.04	4.11	4.19	2.05	0.69	1.39	1.44	1.28	1.35	2.96	1.55	1.62	3.19	4.78
<b>MnO</b>	0.07	0.06	0.05	0.04	0.04	0.04	0.04	0.01	0.01	0.01	0.01	0.01	0.02	0.03	0.04	0.08	0.08
<b>MgO</b>	1.35	0.78	1.16	0.78	1.33	1.34	0.43	0.08	0.15	0.16	0.06	0.05	0.36	0.19	0.08	1.15	1.58
<b>CaO</b>	0.21	0.53	1.78	1.22	1.44	1.58	0.62	0.32	0.25	0.15	0.20	0.35	0.61	0.38	0.17	3.05	2.70
<b>Na<sub>2</sub>O</b>	4.07	1.67	3.40	3.33	2.78	2.93	2.87	3.04	1.71	1.58	2.91	3.35	2.89	2.57	2.53	3.85	3.43
<b>K<sub>2</sub>O</b>	2.84	2.91	2.71	4.35	4.68	4.03	4.55	4.79	7.84	7.43	5.16	4.91	5.47	4.94	5.36	2.26	2.96
<b>P<sub>2</sub>O<sub>5</sub></b>	0.17	0.24	0.20	0.21	0.2	0.19	0.18	0.15	0.05	0.05	0.03	0.04	0.12	0.11	0.07	0.15	0.14
<b>L.O.I.</b>	2.03	2.60	1.50	1.2	1.3	1.2	1.2	1.1	0.4	0.7	0.9	0.8	1.1	0.9	1.4	0.90	0.70
<b>Total</b>	99.05	99.42	99.42	99.51	99.30	99.39	99.73	99.90	99.69	99.79	99.78	99.78	99.47	99.75	99.78	99.97	99.37
<b>As</b>	77.20	1.70	6.80	2.50	6.00	1.80	1.90	0.70	1.00	0.50	2.80	1.10	1.80	101.10	4.00	5.00	5.00
<b>Ba</b>	742.50	388.00	398.00	499	1050	767	256	60	467	109	21	27	784	194	192	689.00	600.00
<b>Be</b>	2.44	3.00	2.00	4.00	2.00	5.00	3.00	6.00	3.00	1.00	9.00	2.00	7.00	3.00	7.00	3.00	5.00
<b>Bi</b>	0.30	0.20	0.10	0.20	0.20	0.20	0.40	0.30	0.10	0.10	0.10	0.10	0.10	0.70	0.40	4.00	4.00
<b>Cd</b>	0.18	0.10	0.10	0.10	0.10	0.10	0.10	0.10	0.10	0.10	0.10	0.10	0.10	0.10	0.10	0.10	0.10
<b>Co</b>	5.84	4.60	6.20	5.20	5.20	5.40	2.70	0.50	1.60	1.00	0.80	0.60	2.30	1.50	1.20	5.00	14.00
<b>Cs</b>	9.79	5.60	4.90	14.30	7.10	6.80	7.30	4.20	3.40	1.60	4.50	4.60	6.40	3.90	4.10	4.20	9.40
<b>Cu</b>	16.34	13.20	10.30	7.20	7.40	10.10	8.70	4.70	4.60	8.20	26.80	2.50	5.00	5.50	5.00	10.00	60.00
<b>Ga</b>	21.03	19.80	18.80	19.10	19.20	18.90	16.70	19.30	14.90	15.30	19.40	19.20	20.70	19.00	19.90	17.00	18.00
<b>Hf</b>	6.40	7.30	6.40	5.00	6.90	5.70	3.10	3.10	4.10	4.30	3.50	3.80	8.80	3.70	5.80	5.90	5.30
<b>Mo</b>	1.20	0.90	1.00	0.60	0.90	0.60	0.30	0.70	0.70	0.70	0.80	0.50	1.70	0.80	1.60	2.00	2.00
<b>Nb</b>	10.49	11.30	11.30	9.60	12.40	11.90	7.90	10.30	7.70	12.10	13.20	13.30	20.20	9.10	20.60	9.00	11.00
<b>Ni</b>	16.56	8.00	7.70	20.00	20.00	20.00	20.00	20.00	20.00	20.00	20.00	20.00	20.00	20.00	20.00	20.00	80.00
<b>Pb</b>	7.94	9.80	22.90	3.50	4.60	5.10	3.60	2.90	7.40	8.60	4.50	5.50	5.10	6.30	5.50	21.00	24.00
<b>Rb</b>	124.40	123.70	137.20	204.6	161.6	142.2	188.2	289.9	206.1	187.4	294.1	275.1	208.7	256.4	227.1	85.00	118.00
<b>Sb</b>	2.27	0.10	0.30	0.10	0.10	0.10	0.10	0.10	0.10	0.10	0.10	0.10	0.10	0.10	0.10	5.00	5.00
<b>Sc</b>	10.00	10.00	6.00	9.00	9.00	4.00	3.00	3.00	4.00	4.00	4.00	4.00	15.00	4.00	8.00	9.00	12.00
<b>Sn</b>	2.11	5.00	5.00	9.00	3.00	3.00	7.00	9.00	4.00	3.00	13.00	15.00	7.00	15.00	12.00	3.00	3.00
<b>Sr</b>	158.00	201.80	83.70	91.20	160.30	150.10	68.70	30.70	73.90	25.20	7.90	8.10	59.90	45.60	25.00	217.00	167.00
<b>Ta</b>	1.07	1.10	1.10	0.80	1.00	0.80	0.70	2.10	0.90	1.10	3.40	1.70	1.60	1.70	2.30	1.00	1.20
<b>Th</b>	11.90	15.70	13.50	11.10	14.40	14.30	5.90	9.10	14.10	17.00	13.50	13.10	22.80	10.20	26.90	13.30	11.50
<b>U</b>	3.70	5.10	4.60	4.10	3.60	3.20	4.80	3.30	2.90	3.20	3.50	3.50	4.60	8.10	4.90	4.50	2.20
<b>V</b>	44.49	49.00	36.00	36.00	63.00	68.00	22.00	8.00	8.00	8.00	8.00	8.00	15.00	8.00	10.00	62.00	53.00
<b>W</b>	1.80	1.90	2.50	3.20	2.60	1.60	3.00	5.60	0.90	2.10	5.20	3.00	2.40	4.40	3.50	1.00	20.00
<b>Y</b>	29.29	43.90	50.60	28.30	38.40	36.20	27.80	28.00	60.10	53.60	44.40	46.00	61.60	31.80	55.80	29.00	24.00
<b>Zn</b>	63.71	52.00	70.00	55.00	71.00	78.00	46.00	7.00	35.00	39.00	15.00	24.00	37.00	30.00	22.00	70.00	70.00
<b>Zr</b>	233.30	263.20	237.10	174.40	249.20	219.10	93.70	73.50	93.80	####	62.20	74.50	311.80	108.10	161.90	245.00	214.00



<b>La</b>	27.90	45.30	38.00	29.60	39.50	38.70	13.60	10.50	22.70	19.50	12.10	13.40	54.20	17.90	31.30	26.90	34.30
<b>Ce</b>	59.00	86.90	75.50	58.10	77.00	78.20	26.70	21.60	42.10	39.70	26.20	29.90	109.80	37.40	97.60	53.20	70.50
<b>Pr</b>	7.26	9.80	8.47	6.99	9.41	9.55	3.36	2.36	4.73	4.85	3.00	3.24	11.94	4.07	6.86	5.88	8.20
<b>Nd</b>	27.83	35.60	31.20	26.00	36.40	36.40	12.60	8.40	16.60	17.10	10.50	10.90	44.70	15.00	24.00	21.60	29.40
<b>Sm</b>	5.80	7.69	7.16	5.70	7.55	7.63	3.15	2.43	4.10	4.41	3.28	3.44	9.37	3.88	4.93	4.70	6.00
<b>Eu</b>	0.98	1.05	1.03	0.87	1.27	1.15	0.41	0.14	0.43	0.13	0.06	0.09	1.17	0.30	0.19	0.95	0.93
<b>Gd</b>	5.22	8.32	7.89	5.59	7.28	7.05	3.38	3.20	5.60	5.50	4.42	4.69	10.60	4.50	6.34	4.00	5.10
<b>Tb</b>	0.87	1.26	1.27	0.89	1.17	1.10	0.67	0.69	1.13	1.18	1.03	1.07	1.70	0.82	1.27	0.70	0.80
<b>Dy</b>	5.30	6.68	8.00	5.09	6.89	6.39	4.59	4.30	7.69	8.23	7.31	7.66	10.28	5.24	9.00	3.70	4.30
<b>Ho</b>	1.06	1.52	1.73	0.99	1.42	1.30	0.98	0.91	1.91	1.91	1.59	1.65	2.13	1.12	2.01	0.70	0.80
<b>Er</b>	2.98	4.52	4.96	2.64	3.92	3.56	3.07	2.85	5.80	6.46	5.35	5.38	6.25	3.64	6.17	2.20	2.10
<b>Tm</b>	0.46	0.60	0.73	0.38	0.57	0.50	0.44	0.43	0.91	1.00	0.85	0.85	0.89	0.52	0.92	0.35	0.32
<b>Yb</b>	3.00	3.98	4.72	2.33	3.56	3.11	2.83	2.95	5.81	6.60	6.10	6.16	5.53	3.70	6.04	2.50	2.20
<b>Lu</b>	0.44	0.58	0.69	0.33	0.53	0.45	0.39	0.44	0.90	0.94	0.92	0.94	0.86	0.56	0.90	0.41	0.36

Longitude: 97°39.5063" E 27°43.71" W 33°29.3112" N 13°50.26" E 33°58.14" E 25°57'58.80" E 21°35.21" E 50°36.95" E 50°35.32" E 50°35.31" E 50°40.64" E 50°35.07" E 50°46.57" E 52°01.84" E 9°48.54.23" E 9°09'32" E  
Latitude: 2°25.2.931" N 2°36.0.93" N 2°32'30.5803" N 34'32.52" N 29.3.27" N 13°34'32.52" N 43°17'45.6" N 54°15.91" N 238.36" S 52°38.37" S 52°36.74" S 52°38.75" S 54°58.32" S 53°56.85" S 53°56.69" N 41°11'04" N 41°11'04" N

1673      **Table 1.** Chemical analyses of magmatic rocks. ICP and ICP–MS methods at ACME–

1674      LABS in Canada.

1675



ZONES	SUBGROUPS	$eNd_{age}$		Tdm (Ga)		$(^{87}\text{Sr}/^{86}\text{Sr})_{age}$	
CIZ & GTMZ	OG	-4,4	-3,8	1,58	2,2	0,709	0,701
	LG	-5,4		4,13		0,664	
	GRA	-1,6		1,59		0,698	
	VOL	-3,6		1,52		0,732	
	OSS	-2,0		1,40		0,711	0,711
PYRENEES	V1	-2,9	-3,6	1,36	1,5		
	G2	-3,8		1,49			
	G3	-4,2		1,50			
	G1	-4,2	-3,7	1,95	1,7		0,701
	CADÍ	-4,1		1,48			
	CASEMÍ	-2,2		1,61		0,696	
	V2	-4,3		1,63		0,705	
Occitan D.	OG-MOD	-3,9	-3,9	1,52	1,5		
	VOL-MOD						
SARDINIA	OG-MOS						
	VOL-MOS						
	OG-USO	-3,9	-3,9	1,52	1,5		
	VOL-UOS						

1678

1679 **Table 2.** Average values of the different subgroups reported in the text.